Table 2 Haplotype structure and frequency in *FCRL3*

Haplotype	Sequence (fcrl3_3-4-5-6)	Frequency: Affected individuals	Frequency: Controls
1	TGGG	0.58	0.65
2	CACA	0.25	0.19
3	CGCA	0.17	0.14

Haplotypes with frequency >0.01 are shown.

P value was still significant when the most conservative Bonferroni correction was applied (comparisons for 507 SNPs; corrected $P = 0.00043$). The four strongly associated SNPs were in LD with each other, and we inferred three common haplotypes (**Table 2**); fcrl3_3, fcrl3_5 and fcrl3_6 showed strong LD with each other ($\Delta > 0.99$), whereas fcrl3_4 showed relatively weak LD with the other three SNPs (mean $\Delta = 0.68$).

To identify causal variants in this segment on the basis of genotype data, we carried out a forward stepwise-regression procedure with a cut-off *P* value to proceed to the next step of 0.01 (ref. 29). No SNP in FCRL genes other than *FCRL3* improved the model. None of the four SNPs in *FCRL3* were preferred over the others in these data (data not shown). This result implied that one of the SNPs in *FCRL3* might cause the disease, but the possibility remained that variants in other genes were truly associated with the disease.

To validate the case-control association test, we evaluated the impact of population stratification on the case-control study (830 cases, 658 controls). We selected 2,069 SNPs, each of which was identified as a tagging SNP[30] in 2,069 distinct LD segments that were previously identified by genotyping 74,842 SNPs distributed in autosomal chromosomes[31]. We analyzed population structure[32] and the χ^2 sum[33] to evaluate stratification but detected no significant evidence of population stratification (**Supplementary Fig. 1** online). These results are suggestive of no or negligible stratification of our samples and support the validity of the case-control association results by removing this confounding factor from further consideration.

Regulatory effect of SNP −169C→T on *FCRL3* expression

Because none of the four SNPs in *FCRL3* (fcrl3_3, fcrl3_4, fcrl3_5 and fcrl3_6) produces amino-acid substitutions, we assessed potential effects of the SNPs on transcription factor binding using TRANSFAC software. Nuclear factor-κB (NF-κB) was predicted to bind the sequence containing the rheumatoid arthritis–susceptibility allele fcrl3_3 (−169C) with a high score (core match 1.000, matrix match 0.957); substitution with the nonsusceptible allele T decreased the score of NF-κB binding substantially (core match 0.760, matrix match 0.824). The other three SNPs were not predicted to bind to any transcriptional factor with high score, and nucleotide substitution was not predicted to affect binding at any regulatory factor. We therefore focused on the 5′ flanking region of fcrl3_3 to explore the regulatory effects on expression of *FCRL3*.

We carried out reporter gene analysis using the genomic sequence of *FCRL3* from nt −523 to +203. We made constructs corresponding to the three haplotypes using SNPs at nt −169 (C→T, fcrl3_3) and −110 (G→A, fcrl3_4; **Fig. 2a**) and used them to transfect Raji cells, a Burkitt's lymphoma cell line that expresses *FCRL3* (ref. 13) and is derived from germinal center B cells. Luciferase activity was substantially greater in cells transfected with −169C −110G or −169C −110A constructs than in cells transfected with −169T −110G constructs. This suggests that SNP −169C→T is crucial for regulation of *FCRL3* expression. To clarify, we cloned single or four tandem copies of 30-bp

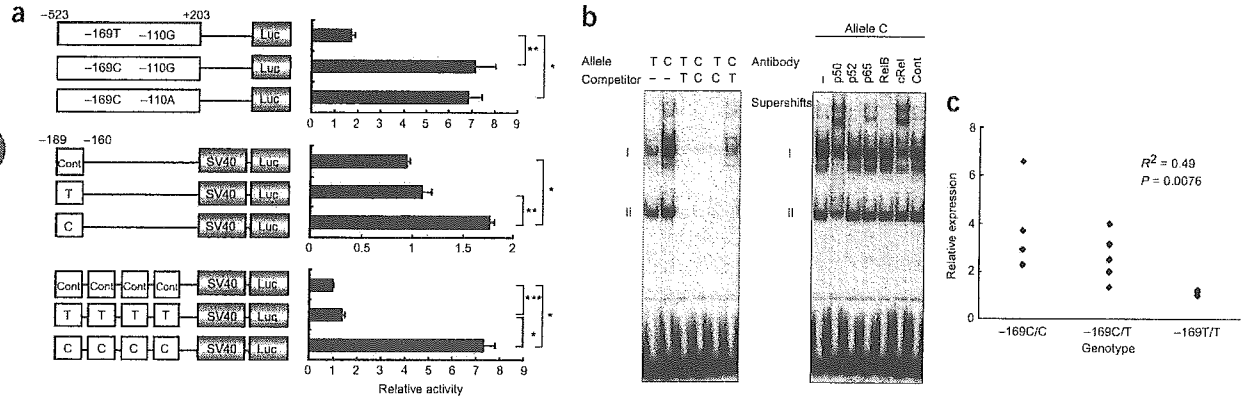

Figure 2 Correlation of *FCRL3* expression with allele and genotype. (**a**) Promoter activity of haplotypes in *FCRL3* (top) and enhancing activity of the 30-bp promoter region around −169C→T (middle and bottom), as evaluated by luciferase assay. Data represent mean ± s.e.m. Representative data from three experiments done in quadruplicate. $^*P < 0.0001$; $^{**}P < 0.001$; $^{***}P < 0.01$ by Student's *t*-test. (**b**) Binding affinity of nuclear factors to the 30-bp promoter region around −169C→T evaluated by EMSA. Allelic difference and competition experiment (left) and supershift experiment using antibodies for NF-κB components (right). (**c**) Expression of *FCRL3* measured by quantitative TaqMan PCR of RNA purified from $CD19^+$ B cells obtained from 13 healthy volunteers (C/C, $n = 4$; C/T, $n = 5$; T/T, $n = 4$). (**d**) ASTQ. *FCRL3* transcripts in B cells and genomic DNA from individuals ($n = 5$) with heterozygous genotypes (−169C/T +358C/G) were amplified and quantified using an *Eag*I restriction-fragment length polymorphism located at position +358. The 122-bp and 85-bp bands represent transcripts of the +358C allele and +358G allele, respectively. Transcripts from homozygous individuals (+358C/C and +358G/G) are shown as controls for digestion.

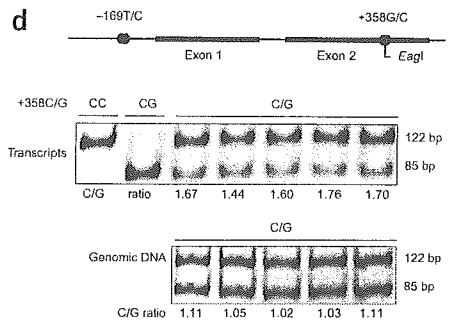

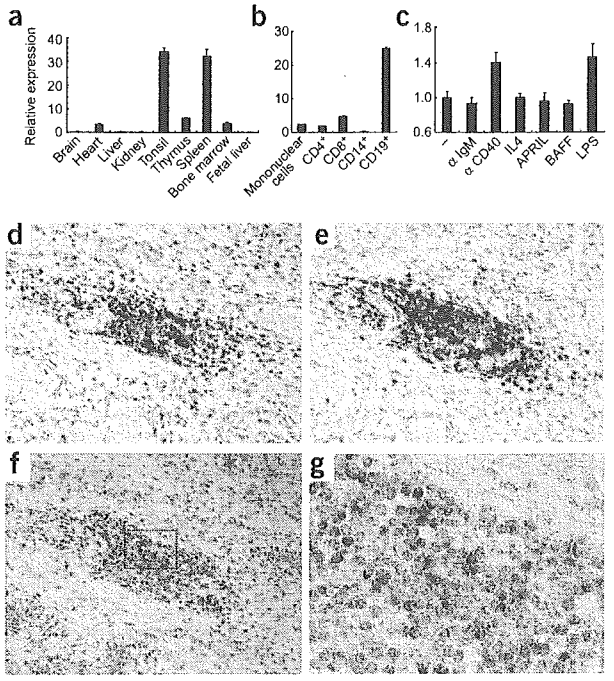

Figure 3 Expression patterns of *FCRL3* in human tissues and cells. (**a**) Relative expression of *FCRL3* in various tissues. (**b**) Relative expression of *FCRL3* in fractionated leukocytes using MTC panel (Clontech). (**c**) Relative expression of *FCRL3* in response to stimuli (antibody to CD40, 1 μg ml^{-1}; antibody to IgM, 1 μg ml^{-1}; IL-4, 10 ng ml^{-1}; APRIL, 10 ng ml^{-1}; BAFF, 10 ng ml^{-1}; LPS, 100 ng ml^{-1}) for 4 h. Representative data from three experiments done in triplicate. (**d**,**e**) Lymphocyte aggregates in rheumatoid arthritis synovium. T cells and B cells in serial sections were immunostained using antibodies to CD3 (**d**) and CD20 (**e**), respectively. (**f**,**g**) *FCRL3* mRNA expression (blue stain) in rheumatoid arthritis synovium as analyzed by *in situ* hybridization. Higher magnification views of synovium (**g**) are denoted by the box in **f** (magnifications: **d**–**f**, ×100; **g**, ×400). Counterstaining: **d**,**e**, hematoxylin; **f**,**g**, nuclear fast red.

oligonucleotides surrounding SNP −169C→T and control oligonucleotides into a vector with the SV40 promoter. Cells transfected with a single copy of the C allele produced substantially greater luciferase activity than cells transfected with a single copy of the T allele. More convincingly, transfection with four tandem copies of the C allele enhanced luciferase activity by a factor of 20 over transfection with four tandem copies of the T allele (**Fig. 2a**).

To elucidate specific nuclear factors that bind the disease-susceptible allele, we analyzed the sequence around −169C→T. These sequences were predicted by TRANSFAC software to have binding affinity for NF-κB, which regulates a wide variety of genes in the immune system. The disease-susceptible sequence (including −169C) had higher matrix similarity to the consensus NF-κB binding motif than the nonsusceptible sequence (including −169T). We then carried out electrophoretic mobility shift assays (EMSAs) to examine whether differences between the susceptible −169C allele and the nonsusceptible −169T allele affected binding of nuclear proteins from Raji cells. We used the same 30-bp labeled oligonucleotides used in the luciferase assay. These sequences contain the predicted NF-κB binding site. We observed two main bands, I and II, in the presence of nuclear extracts; the intensity of band I was higher for the susceptible −169C allele than for the nonsusceptible −169T allele (**Fig. 2b**). Competition assays with unlabeled oligonucleotides indicated that these complexes were specific for the probes. In addition, competition assays with unlabeled probes of the C allele for T and the T allele for C showed that the C allele was better able to compete for binding, a result consistent with the higher binding affinity of labeled C allele probes alone. We also carried out a supershift experiment with antibodies specific for NF-κB components (p50, p52, p65, RelB and cRel). We observed supershifts in some lanes with specific antibodies for p50, p65 and cRel (**Fig. 2b**). Among these, only antibody to p50 shifted band II, suggestive of the presence of a p50-p50 homodimer. Band I had the highest intensity and a substantial allelic difference and was supershifted by antibodies to p50, p65 and cRel. Although these findings indicate that band I comprises a mixture of heterodimers, the greater shifts caused by antibodies to p50 and cRel suggest that the main component is a p50-cRel heterodimer.

The two *in vitro* assays showed the potent transcriptional activity of the disease-susceptible haplotype regulated by NF-κB, suggesting that expression of *FCRL3* is greater from the disease-susceptible −169C allele than from the nonsusceptible −169T allele. To extend these findings, we quantified expression of *FCRL3* in peripheral blood B cells from healthy donors using quantitative TaqMan methods and analyzed the effect of the number of susceptible copies on the transcript level by regression model. Regression analysis identified a significant positive correlation between number of susceptible chromosomes and transcription level ($R^2 = 0.49$, $P = 0.0076$; **Fig. 2c**).

We also carried out allele-specific transcript quantification[9,34] to confirm the effect of the SNP on transcription. Using an *Eag*I restriction-fragment length polymorphism located at position +358 in exon 2 of *FCRL3* (fcrl3_5, +358C→G), we measured the relative contribution of each haplotype to transcript production in heterozygous individuals (**Fig. 2d**). We evaluated the transcripts of five doubly heterozygous individuals with genotype −169C/T +358C/G; the mean ratio (susceptible versus nonsusceptible haplotype) was 1.63, significantly higher than that of DNA amplicons (ratio = 1.06, $P < 1 \times 10^{-5}$) from the same individuals. (The quantity of template DNA from the two haplotypes was equal.) These results show that the

Table 3 Genotype and autoantibodies in individuals with rheumatoid arthritis

	RF		Antibody to CCP	
Genotype	n^a	Serum level[b] (IU/ml)	n^c	Positivity (%)
−169C/C	29	479.9 ± 91.3[d]	17	100.0[e]
−169C/T	75	323.7 ± 47.3[d]	35	94.3[e]
−169T/T	44	216.4 ± 44.0[d]	19	73.7[e]

[a]$N = 148$. [b]Mean ± s.e.m. [c]$N = 71$. [d]$R^2 = 0.049$, $P = 0.0065$ by regression analysis. [e]$P = 0.029$ by Fisher's exact test.

Table 4 Association of SNP −169C→T with AITD and SLE

Disease	*n*	Genotype CC	CT	TT	Allele C frequency	Recessive-trait comparison OR (95% c.i.)	χ^2	*P*
GD	351	72	179	100	0.46	1.79 (1.34–2.39)	15.7	0.000074
HT	158	30	74	54	0.42	1.62 (1.07–2.47)	5.2	0.022
AITD total	509	102	253	154	0.45	1.74 (1.35–2.24)	18.5	0.000017
SLE	564	100	259	205	0.41	1.49 (1.16–1.92)	9.8	0.0017
RA* + AITD + SLE	2,437	438	1,167	832	0.42	1.52 (1.29–1.79)	24.2	0.00000084
Control	2,037	257	995	785	0.37			

*Rheumatoid arthritis represents sum of three sets (n = 1,364). c.i., confidence interval; GD, Graves' disease; HT, Hashimoto's thyroiditis; OR, odds ratio; RA, rheumatoid arthritis.

expression of *FCRL3* is higher in individuals with the disease-susceptible haplotype and suggest that higher expression of *FCRL3* is a potential cause and component of the pathological mechanism(s) leading to rheumatoid arthritis.

Expression of *FCRL3* mRNA

We then quantified *FCRL3* expression in multiple tissues using TaqMan methods. Expression of *FCRL3* transcripts was high in the spleen and tonsils (**Fig. 3a**), which are secondary lymphoid organs. We observed lower expression in thymus and bone marrow. In human blood fractions, $CD19^+$ cells, which represent the B-cell population, had the greatest *FCRL3* expression among peripheral blood mononuclear cells. $CD4^+$ and $CD8^+$ cells had less expression (**Fig. 3b**). We next examined the effect of B-cell stimulation on *FCRL3* expression. We cultured peripheral blood B cells from a healthy donor for 4 h using known B-cell stimulants and then quantified *FCRL3* mRNA (**Fig. 3c**). Expression of *FCRL3* was increased by antibody to CD40 and lipopolysaccharide (LPS).

We then investigated expression of *FCRL3* transcripts in synovial tissue using *in situ* hybridization methods. T and B cells are the key players with regard to inflammation in synovial tissue, producing proinflammatory cytokines and autoantibodies that might be pathogenic[1]. These cells show three distinct histological patterns: diffuse infiltration, clustering in aggregates and follicles with germinal-center reaction[35,36]. We observed aggregations of T and B cells in paraffin-embedded synovial sections from individuals with rheumatoid arthritis, using immunostaining with antibodies to CD3 and CD20, respectively (**Fig. 3d,e**). *In situ* hybridization assay with serial sections detected *FCRL3* mRNA in aggregated lymphocytes (**Fig. 3f,g**). Although strict differentiation between B and T cells was difficult, at least some aggregated B cells were positive, with strong expression of *FCRL3* mRNA. Synovium from two other individuals with rheumatoid arthritis had similar lymphocyte aggregates and *FCRL3* expression (**Supplementary Fig. 2** online).

SNP association with autoantibody and *HLA-DRB1* status

Because we suspected that higher *FCRL3* expression led to B-cell abnormalities in rheumatoid arthritis, we examined associations in individuals with rheumatoid arthritis between genotype and two rheumatoid arthritis–related autoantibodies: rheumatoid factor (RF) and antibody to cyclic citrullinated peptide (CCP). RF is a well-known autoantibody for the Fc region of IgG, and titers correlate with rheumatoid arthritis disease activity[37]. Antibody to CCP recognizes peptides containing citrulline and is detected in rheumatoid arthritis with extremely high specificity[38,39]. RF titer in individuals with rheumatoid arthritis was significantly positively correlated with the number of susceptible alleles (R^2 = 0.049, P = 0.0065; **Table 3**). The positive ratio of antibody to CCP in individuals with rheumatoid arthritis also differed significantly among genotypes ($P < 0.05$) and correlated with number of susceptible alleles.

Because genetic interactions between HLA and non-HLA loci have been described in susceptibility for rheumatoid arthritis and other autoimmune diseases[26,40], we compared genotype distributions for SNP −169C→T among three rheumatoid arthritis subgroups stratified by number of *HLA-DRB1* shared-epitope alleles. We previously genotyped *HLA-DRB1* in our population and observed significant associations between rheumatoid arthritis susceptibility and shared-epitope alleles[4]. Allele frequency of the rheumatoid arthritis–susceptibility allele −169C was significantly higher in the subgroup with two copies of shared-epitope alleles (0.49, n = 113) than in the subgroup with no shared-epitope alleles (0.39, n = 215; $P < 0.05$).

Replication study of association in three autoimmunities

To confirm associations between the *FCRL3* variant and rheumatoid arthritis susceptibility, we carried out a replication study (540 individuals with rheumatoid arthritis, 636 controls). We compared allele frequency and found a significant association between fcrl3_3 (−169C→T) and rheumatoid arthritis susceptibility (allele frequency was 0.40 in individuals with rheumatoid arthritis versus 0.46 in controls; P = 0.041; **Supplementary Table 2** online). We noted no significant differences between two cohorts that consisted of the replication samples. These results further confirmed the association of the fcrl3_3 −169C allele with rheumatoid arthritis susceptibility in Japanese individuals.

Because this region is associated with multiple autoimmune diseases, and because several variants are involved in multiple autoimmunities, we investigated associations between SNP −169C→T and two other autoimmune diseases: AITD and SLE. We recruited 509 Japanese individuals with AITD (351 with Graves' disease and 158 with Hashimoto's thyroiditis) and 564 Japanese individuals with SLE and compared them with 2,037 Japanese controls. In addition, we combined AITD, SLE and rheumatoid arthritis cases as subjects with an autoimmune phenotype and tested for associations with the SNP. Individual diseases, as well as combination of two AITDs and combination of AITD, SLE and rheumatoid arthritis, were significantly associated with the SNP (odds ratio = 1.52, P = 0.00000084 in Japanese for a recessive model between all four autoimmunities considered in aggregate and controls; **Table 4**). As rheumatoid arthritis–specific autoantibodies were correlated with the number of susceptible alleles, antibody to DNA titer was higher in individuals with SLE with genotype −169C/C than in subjects with other genotypes (294.1 IU ml^{-1} versus 145.5 IU ml^{-1}; n = 120; P = 0.026 by Student's t-test), a conclusion not further established by regression analysis (P = 0.12).

DISCUSSION

LD mapping of 1q21–23 in Japanese subjects identified multiple LD blocks in the region, and one block containing *FCRL3* was associated with rheumatoid arthritis. This association was replicated in a second Japanese case-control set. The rheumatoid arthritis–associated allele was also associated with increased risk of other autoimmune disorders, such as AITD (Graves' disease and Hashimoto's thyroiditis) and SLE. Recent reports on autoimmune disease–associated polymorphisms show that some disease-susceptible variants are limited to specific ethnic groups[12] whereas others are widely dispersed but significantly associated with disease in only specific ethnic groups[41,42]. We evaluated four-SNP haplotypes in *FCRL3* in African American, European American and Asian (Korean and Japanese) subjects and found weaker LD in African Americans than in other groups and substantial differences in allelic frequency among the groups (**Supplementary Table 3** online).

Although the evidence presented here for *FCRL3* being an autoimmune disease–susceptibility gene is powerful, additional autoimmune disease–related genes probably exist in this region. For example, 1q23 is a good candidate locus for SLE susceptibility[6], particularly involving the association of the classical FcγR genes with SLE susceptibility in the Japanese population[19], although those variants are not in LD with SNP −169C→T in our Japanese subjects ($\Delta < 0.05$, **Fig. 1a**). Multiple SLE susceptibility genes are also homologous to human 1q23 in mouse models of SLE[43].

Further evaluation of polymorphism associations showed that a SNP in the promoter region of *FCRL3* alters expression of *FCRL3* through NF-κB binding. Because higher expression of *FCRL3* was observed in individuals with susceptible alleles, and augmented autoantibody production was associated with the susceptible genotype, important steps in the sequence of events leading to autoimmunity must proceed through *FCRL3*. That the susceptible allele is associated with *HLA-DRB1* in rheumatoid arthritis is consistent with *FCRL3* functioning in the context of HLA class II restriction, which is usually seen in the interaction between T cells and antigen-presenting cells, including B cells. Moreover, together with the dominant expression of *FCRL3* on B cells and the importance of B cells suggested by a recent clinical trial of B cell–depleting therapy[44], the present findings might provide a genetic basis for B-cell abnormality in autoimmunity.

Although the precise function of *FCRL3* is unknown, its predicted molecular structure suggests that it is a membranous protein that conveys signals into cells through a cytoplasmic domain containing an immunoreceptor-tyrosine activation motif and an immunoreceptor-tyrosine inhibitory motif[14]. An *in vitro* study showing the binding of tyrosine kinases syk and ZAP70 to the immunoreceptor-tyrosine activation motif region and of tyrosine phosphatases SHP-1 and SHP-2 to the immunoreceptor-tyrosine inhibitory motif region[17] supports the proposed signaling function of *FCRL3*. In a previous study examining *in situ* hybridization in human tonsil, *FCRL3* was expressed in the germinal center, with particularly high expression in the light zone[16], suggesting that *FCRL3* functions predominantly in centrocytes. The present finding that CD40 stimulation, which is important in germinal-center formation[45], upregulates *FCRL3* expression in B cells could indicate that *FCRL3* is specifically expressed in germinal-center centrocytes under the influence of CD40 signals. In the light zone, centrocytes undergo clonal selection and affinity maturation regulated by positive and negative signals from antigen receptors and coreceptors[46]. High expression of *FCRL3* and augmented autoantibody production in individuals with the disease-susceptible genotype is consistent with the idea that *FCRL3* influences the fate of B cells and augments the emergence of self-reactive cells in the germinal center.

In addition to its role in lymphoid tissues, expression of *FCRL3* in synovial tissue might explain the pathological connection between *FCRL3* variants and rheumatoid arthritis. *FCRL3* is strongly expressed in aggregated lymphocytes. Although our synovial samples showed only T-cell–B-cell aggregates, lymphocytes in rheumatoid arthritis synovial tissue are known to form a germinal center–like structure, called an ectopic germinal center, where T cell–dependent antibody production and affinity maturation occur[36]. Ectopic germinal-center formation also occurs in tissues from individuals with AITD and SLE, and *FCRL3* might be involved in pathological autoimmune reaction in these disease-specific ectopic lymphocyte aggregates.

Considering that augmented expression of *FCRL3* is associated with susceptibility to autoimmune disorders, and that *FCRL3* expression is regulated in B cells in the secondary lymphoid organ and is detected in lymphocytes of disease-specific tissues, *FCRL3* probably functions in immunity and potentially pathogenic in autoimmune disorders.

METHODS

Subjects. We enrolled three independent cohorts of individuals with rheumatoid arthritis (n = 830, 217 and 323), a cohort of individuals with SLE (n = 564) and a cohort of individuals with AITD (n = 509) comprising Graves' disease (n = 351) and Hashimoto's thyroiditis (n = 158) through several medical institutes in Japan. We recruited four independent cohorts of unaffected control subjects (n = 658, 262, 374 and 752) at various sites in Japan. All subjects were Japanese. Individuals with rheumatoid arthritis (84.2% women; age 59.0 ± 12.3 years (mean ± s.d.); 75.0% RF-positive) satisfied the revised criteria of the American Rheumatism Association for rheumatoid arthritis[47]. Individuals with SLE satisfied the criteria of the American College of Rheumatology for SLE[48]. Diagnosis of AITD was established on the basis of clinical findings and results of routine examinations for circulating thyroid hormone and thyroid-stimulating hormone concentrations, serum levels of antibodies against thyroglobulin, thyroid microsomes and thyroid-stimulating hormone receptors, ultrasonography, $^{[99m]}TCO_4^-$ (or $^{[123]}I$) uptake and thyroid scintigraphy.

We evaluated LD at 1q21–23 in the first control cohort compared with the first rheumatoid arthritis cohort to identify the rheumatoid arthritis–associated LD block and SNPs. The second and third rheumatoid arthritis and control cohorts were used for replication testing of results from the first cohorts. We tested Graves' disease; Hashimoto's thyroiditis; SLE; the combination of the two AITDs; and the combination of rheumatoid arthritis, SLE and the two AITDs for associations using the total pool of controls. We enrolled control subjects from three other ethnic groups, Korean (n = 100), African American (n = 120) and European American (n = 120), for evaluation of *FCRL3* haplotypes. We sampled synovial tissues from individuals with rheumatoid arthritis who underwent arthroplastic surgery. All subjects provided informed consent to participate in the study, as approved by the ethical committee of the SNP Research Center, RIKEN.

SNPs and genotyping. We identified SNPs in exons and 5′ and 3′ flanking regions of *FCRL1*, *FCRL2*, *FCRL3* and *FCRLψ4* by direct sequencing of DNA from 24 individuals. We selected other SNPs from the JSNP and Assay-On-Demand SNP databases (Applied Biosystems). We genotyped SNPs using Invader and TaqMan assays[41] as indicated by the manufacturers. Probe sets for the Invader assay were designed and synthesized by Third Wave Technologies, and those for the TaqMan assay were obtained from Applied Biosystems. When assessing the results of SNP genotyping, we generally excluded successful call rates <0.95 and values of $P < 0.01$ obtained by Hardy-Weinberg equilibrium testing in control subjects. The error rate of Invader assay was 0.0023, which was estimated by 11,092 assays in two replicates using 118 randomly selected SNPs (internal control data).

Luciferase assay. We cloned the promoter fragment of three haplotypes corresponding to nt −523 to +203 of *FCRL3* into the pGL3-Basic vector (Promega). We generated oligonucleotides using the allelic sequences of nt −189 to −160 of *FCRL3*. We cloned a single copy or four tandem copies of

these oligonucleotides into pGL3-Promoter vector (Promega). We grew Raji cells (RCB1647; RIKEN Cell Bank) in RPMI1640 medium supplemented with 10% fetal bovine serum and antibiotics. We electroporated (230 V and 975 μF) 1×10^7 cells with 5 pmol of constructs and 1 pmol of pRL-TK vector (internal control for transfection efficiency) in a 0.4-cm gap cuvette. After 48 h, we collected cells and measured luciferase activity using the Dual-Luciferase Reporter Assay System (Promega).

EMSA. We carried out EMSA and preparation of nuclear extract from Raji cells as previously described[49]. We labeled oligonucleotides −169T and −169C with digoxigenin -11-ddUTP using the DIG gel-shift kit (Roche). We incubated 5 μg of nuclear extract with 40 fmol of digoxigenin-labeled nucleotide for 25 min at room temperature. For competition experiments, we preincubated nuclear extract with unlabeled oligonucleotide (100-fold excess) before adding digoxigenin-labeled oligonucleotide. For supershift assays, we incubated 4 μg of antibodies to p50, p52, p65, RelB or cRel and rabbit IgG (control antibody; Santa Cruz Biotechnology) for 15 min at room temperature after incubation of the labeled probe. We separated protein-DNA complexes on a nondenaturing 6% polyacrylamide gel in 0.5× Tris-Borate-EDTA buffer. We transferred the gel to a nitrocellulose membrane and detected signals using an LAS-3000 luminoimage analyzer (Fujifilm).

RNA extraction and cDNA preparation. We collected peripheral blood from healthy volunteers to obtain $CD19^+$ lymphocytes. We separated polymorphonuclear cells by differential centrifugation using Lymphoprep resolving solution (AXIS-FIELD). We isolated $CD19^+$ lymphocytes using the MACS system with CD19 microbeads (Miltenyi Biotec) and confirmed that cell purity was >95% using flow cytometry. We stimulated cells with antibodies to CD40 (Cymbus Biotechnology) or IgM (Jackson Immunoresearch), with Il-4 (eBioscience), with APRIL (PeproTech), with BAFF (PeproTech) or with LPS (Sigma) for 4 h. We isolated total RNA using RNeasy Mini Kit (Qiagen). We quantified RNA in other normal tissues using Premium Total RNA (Clontech). We reverse-transcribed total RNA using TaqMan Gold RT-PCR reagents with random hexamers (Applied Biosystems) in accordance with the instructions of the manufacturer.

Quantification of *FCRL3* expression using real-time RT-PCR. We carried out real-time quantitative PCR using an ABI PRISM 7900 (Applied Biosystems) and Assay-on-Demand TaqMan probe and primers (Hs00364720_m1 for *FCRL3*) in accordance with the manufacturer's instructions. We generated a standard curve from the amplification data for *FCRL3* primers using a dilution series of total RNA from Raji cells as templates and normalized data to GUS level.

ASTQ. We carried out ASTQ as previously described[34] with some modifications. We prepared cDNA from B cells as described above. We amplified both cDNA and genomic DNA by PCR for 37 cycles using primers specific for exon 2 of *FCRL3* (**Supplementary Table 4** online) and for an additional cycle using forward primer with Alexa Fluor 488 label at the 5′ end. Products were directly digested using *EagI* by incubation at 37 °C for 12 h. We monitored full digestion by the inclusion of PCR products from +358G/G homozygotes. We then separated digested products on a 12.5% polyacrylamide gel and quantified them using an LAS-3000 analyzer.

***In situ* hybridization and immunohistochemistry.** We carried out *in situ* hybridization as previously described[50]. We obtained probes from PCR products using the sequence of *FCRL3* (nt 2052–2490, comprising the intracellular unique region that is poorly conserved among members of this family). An additional probe of the 5′ untranslated sequence yielded similar results. We also examined control probes, which yielded no specific hybridization (data not shown). We used antibodies to CD3 (clone PS-1, Nichirei) and CD20 (clone L26, Zymed) for immunohistochemistry with an ABC Elite kit (Vector Labs) in accordance with the manufacturer's instructions. No specific staining was detected using mouse isotype IgG (data not shown).

Measurement of autoantibodies. We measured RF in sera of individuals with rheumatoid arthritis using latex-enhanced immunonephelometric assay. We measured antibody to DNA in sera of individuals with SLE by radioimmunoassay. Individuals with rheumatoid arthritis (n = 147, 81.1% women; age 63.9 ± 10.6 years (mean ± s.d.); 87.8% RF-positive; mean Steinbrocker radiographic stage 3.2) or SLE (n = 120, 92.6% women; age 36.6 ± 12.7 years (mean ± s.d.)) were part of the cohorts or from a single medical institute, respectively. For each individual, we used the maximum value of RF and antibody to DNA measured during the treatment period in the medical center or outpatient clinic. We detected antibody to CCP at a single time point using enzyme-linked immunosorbent assay, as previously described[38].

Statistical analysis. We calculated LD index Δ (ref. 28) and drew **Figure 1a** using Excel software (Microsoft). We estimated haplotype frequencies using HAPLOTYPER software. We applied the χ^2 test for contingency table tests for associations between allele-genotype distribution and phenotypes. *FCRL3* expression in B cells and autoantibody production were regressed on the number of susceptible alleles (coded 0, 1 and 2). All other statistical analyses, unless otherwise stated, were done using STATISTICA software (StatSoft).

URLs. The JSNP database is available at http://snp.ims.u-tokyo.ac.jp/index.html. TRANSFAC is available at http://www.gene-regulation.com/. HAPLOTYPER is available at http://www.people.fas.harvard.edu/~junliu/Haplo/docMain.htm.

GenBank accession number. *FCRL3* mRNA, NM_052939.

Note: Supplementary information is available on the Nature Genetics website.

ACKNOWLEDGMENTS

We thank E. Kanno and other members of the Laboratory for Rheumatic Diseases for technical assistance; H. Kawakami for expertise in computer programming; M. Yukioka, S. Tohma, Y. Nishioka, T. Matsubara, S. Wakitani, R. Teshima, N. Ishikawa, K. Ito, K. Ito, K. Kuma, H. Tamai and T. Akamizu for clinical sample collection; M. Ishikawa and Y. Amasaki for preparation of the second population study; M. Nagashima and S. Yoshino for sampling rheumatoid arthritis synovium; and K. Nagatani and Y. Komagata for advice. This work was supported by grants from the Japanese Millennium Project, the US National Institutes of Health and the Korean Molecular and Cellular BioDiscovery Research Program.

COMPETING INTERESTS STATEMENT

The authors declare that they have no competing financial interests.

Received 20 December 2004; accepted 25 February 2005
Published online at http://www.nature.com/naturegenetics/

1. Firestein, G.S. Evolving concepts of rheumatoid arthritis. *Nature* **423**, 356–361 (2003).
2. Gregersen, P.K., Silver, J. & Winchester, R.J. The shared epitope hypothesis. An approach to understanding the molecular genetics of susceptibility to rheumatoid arthritis. *Arthritis Rheum.* **30**, 1205–1213 (1987).
3. Newton, J.L., Harney, S.M., Wordsworth, B.P. & Brown, M.A. A review of the MHC genetics of rheumatoid arthritis. *Genes Immun.* **5**, 151–157 (2004).
4. Kochi, Y. *et al.* Analysis of single-nucleotide polymorphisms in Japanese rheumatoid arthritis patients shows additional susceptibility markers besides the classic shared epitope susceptibility sequences. *Arthritis Rheum.* **50**, 63–71 (2004).
5. Seldin, M.F., Amos, C.I., Ward, R. & Gregersen, P.K. The genetics revolution and the assault on rheumatoid arthritis. *Arthritis Rheum.* **42**, 1071–1079 (1999).
6. Tsao, B.P. The genetics of human systemic lupus erythematosus. *Trends Immunol.* **24**, 595–602 (2003).
7. Bowcock, A.M. & Cookson, W.O. The genetics of psoriasis, psoriatic arthritis and atopic dermatitis. *Hum. Mol. Genet.* **13** Suppl 1, R43–R55 (2004).
8. Marrack, P., Kappler, J. & Kotzin, B.L. Autoimmune disease: why and where it occurs. *Nat. Med.* **7**, 899–905 (2001).
9. Ueda, H. *et al.* Association of the T-cell regulatory gene CTLA4 with susceptibility to autoimmune disease. *Nature* **423**, 506–511 (2003).
10. Becker, K.G. *et al.* Clustering of non-major histocompatibility complex susceptibility candidate loci in human autoimmune diseases. *Proc. Natl. Acad. Sci. USA* **95**, 9979–9984 (1998).
11. Tokuhiro, S. *et al.* An intronic SNP in a RUNX1 binding site of SLC22A4, encoding an organic cation transporter, is associated with rheumatoid arthritis. *Nat. Genet.* **35**, 341–348 (2003).
12. Begovich, A.B. *et al.* A missense single-nucleotide polymorphism in a gene encoding a protein tyrosine phosphatase (PTPN22) is associated with rheumatoid arthritis. *Am. J. Hum. Genet.* **75**, 330–337 (2004).
13. Davis, R.S., Wang, Y.H., Kubagawa, H. & Cooper, M.D. Identification of a family of Fc receptor homologs with preferential B cell expression. *Proc. Natl. Acad. Sci. USA* **98**, 9772–9777 (2001).

14. Davis, R.S. *et al.* Fc receptor homologs: newest members of a remarkably diverse Fc receptor gene family. *Immunol. Rev.* **190**, 123–136 (2002).
15. Hatzivassiliou, G. *et al.* IRTA1 and IRTA2, novel immunoglobulin superfamily receptors expressed in B cells and involved in chromosome 1q21 abnormalities in B cell malignancy. *Immunity* **14**, 277–289 (2001).
16. Miller, I., Hatzivassiliou, G., Cattoretti, G., Mendelsohn, C. & Dalla-Favera, R. IRTAs: a new family of immunoglobulinlike receptors differentially expressed in B cells. *Blood* **99**, 2662–2669 (2002).
17. Xu, M.J., Zhao, R., Cao, H. & Zhao, Z.J. SPAP2, an Ig family receptor containing both ITIMs and ITAMs. *Biochem. Biophys. Res. Commun.* **293**, 1037–1046 (2002).
18. Ravetch, J.V. & Bolland, S. IgG Fc receptors. *Annu. Rev. Immunol.* **19**, 275–290 (2001).
19. Kyogoku, C. *et al.* Fcgamma receptor gene polymorphisms in Japanese patients with systemic lupus erythematosus: contribution of FCGR2B to genetic susceptibility. *Arthritis Rheum.* **46**, 1242–1254 (2002).
20. Capon, F. *et al.* Fine mapping of the PSORS4 psoriasis susceptibility region on chromosome 1q21. *J. Invest. Dermatol.* **116**, 728–730 (2001).
21. Dai, K.Z. *et al.* The T cell regulator gene SH2D2A contributes to the genetic susceptibility of multiple sclerosis. *Genes Immun.* **2**, 263–268 (2001).
22. Jirholt, J. *et al.* Genetic linkage analysis of collagen-induced arthritis in the mouse. *Eur. J. Immunol.* **28**, 3321–3328 (1998).
23. Sundvall, M. *et al.* Identification of murine loci associated with susceptibility to chronic experimental autoimmune encephalomyelitis. *Nat. Genet.* **10**, 313–317 (1995).
24. Teuscher, C. *et al.* Evidence that Tmevd2 and eae3 may represent either a common locus or members of a gene complex controlling susceptibility to immunologically mediated demyelination in mice. *J. Immunol.* **159**, 4930–4934 (1997).
25. Podolin, P.L. *et al.* Congenic mapping of the insulin-dependent diabetes (Idd) gene, Idd10, localizes two genes mediating the Idd10 effect and eliminates the candidate Fcgr1. *J. Immunol.* **159**, 1835–1843 (1997).
26. Nieto, A. *et al.* Involvement of Fcgamma receptor IIIA genotypes in susceptibility to rheumatoid arthritis. *Arthritis Rheum.* **43**, 735–739 (2000).
27. Radstake, T.R. *et al.* Role of Fcgamma receptors IIA, IIIA, and IIIB in susceptibility to rheumatoid arthritis. *J. Rheumatol.* **30**, 926–933 (2003).
28. Devlin, B. & Risch, N. A comparison of linkage disequilibrium measures for fine-scale mapping. *Genomics* **29**, 311–322 (1995).
29. Cordell, H.J. & Clayton, D.G. A unified stepwise regression procedure for evaluating the relative effects of polymorphisms within a gene using case/control or family data: application to HLA in type 1 diabetes. *Am. J. Hum. Genet.* **70**, 124–141 (2002).
30. Sebastiani, P. *et al.* Minimal haplotype tagging. *Proc. Natl. Acad. Sci. USA* **100**, 9900–9905 (2003).
31. Tsunoda, T. *et al.* Variation of gene-based SNPs and linkage disequilibrium patterns in the human genome. *Hum. Mol. Genet.* **13**, 1623–1632 (2004).
32. Pritchard, J.K., Stephens, M. & Donnelly, P. Inference of population structure using multilocus genotype data. *Genetics* **155**, 945–959 (2000).
33. Pritchard, J.K. & Rosenberg, N.A. Use of unlinked genetic markers to detect population stratification in association studies. *Am. J. Hum. Genet.* **65**, 220–228 (1999).
34. Kaijzel, E.L. *et al.* Allele-specific quantification of tumor necrosis factor alpha (TNF) transcription and the role of promoter polymorphisms in rheumatoid arthritis patients and healthy individuals. *Genes Immun.* **2**, 135–144 (2001).
35. Takemura, S. *et al.* Lymphoid neogenesis in rheumatoid synovitis. *J. Immunol.* **167**, 1072–1080 (2001).
36. Weyand, C.M. & Goronzy, J.J. Ectopic germinal center formation in rheumatoid synovitis. *Ann. N. Y. Acad. Sci.* **987**, 140–149 (2003).
37. Alarcon, G.S. *et al.* Suppression of rheumatoid factor production by methotrexate in patients with rheumatoid arthritis. Evidence for differential influences of therapy and clinical status on IgM and IgA rheumatoid factor expression. *Arthritis Rheum.* **33**, 1156–1161 (1990).
38. Suzuki, K. *et al.* High diagnostic performance of ELISA detection of antibodies to citrullinated antigens in rheumatoid arthritis. *Scand. J. Rheumatol.* **32**, 197–204 (2003).
39. Rantapaa-Dahlqvist, S. *et al.* Antibodies against cyclic citrullinated peptide and IgA rheumatoid factor predict the development of rheumatoid arthritis. *Arthritis Rheum.* **48**, 2741–2749 (2003).
40. Capon, F., Semprini, S., Dallapiccola, B. & Novelli, G. Evidence for interaction between psoriasis-susceptibility loci on chromosomes 6p21 and 1q21. *Am. J. Hum. Genet.* **65**, 1798–1800 (1999).
41. Suzuki, A. *et al.* Functional haplotypes of PADI4, encoding citrullinating enzyme peptidylarginine deiminase 4, are associated with rheumatoid arthritis. *Nat. Genet.* **34**, 395–402 (2003).
42. Barton, A. *et al.* A functional haplotype of the PADI4 gene associated with rheumatoid arthritis in a Japanese population is not associated in a United Kingdom population. *Arthritis Rheum.* **50**, 1117–1121 (2004).
43. Jorgensen, T.N., Gubbels, M.R. & Kotzin, B.L. New insights into disease pathogenesis from mouse lupus genetics. *Curr. Opin. Immunol.* **16**, 787–793 (2004).
44. Edwards, J.C. *et al.* Efficacy of B-cell-targeted therapy with rituximab in patients with rheumatoid arthritis. *N. Engl. J. Med.* **350**, 2572–2581 (2004).
45. Gray, D. *et al.* Observations on memory B-cell development. *Semin. Immunol.* **9**, 249–254 (1997).
46. van Eijk, M., Defrance, T., Hennino, A. & de Groot, C. Death-receptor contribution to the germinal-center reaction. *Trends Immunol.* **22**, 677–682 (2001).
47. Arnett, F.C. *et al.* The American Rheumatism Association 1987 revised criteria for the classification of rheumatoid arthritis. *Arthritis Rheum.* **31**, 315–324 (1988).
48. Hochberg, M.C. Updating the American College of Rheumatology revised criteria for the classification of systemic lupus erythematosus. *Arthritis Rheum.* **40**, 1725 (1997).
49. Aikawa, Y., Yamamoto, M., Yamamoto, T., Morimoto, K. & Tanaka, K. An anti-rheumatic agent T-614 inhibits NF-kappaB activation in LPS- and TNF-alpha-stimulated THP-1 cells without interfering with IkappaBalpha degradation. *Inflamm. Res.* **51**, 188–194 (2002).
50. Hoshino, M. *et al.* Identification of the stef gene that encodes a novel guanine nucleotide exchange factor specific for Rac1. *J. Biol. Chem.* **274**, 17837–17844 (1999).

Rheumatology 2005;44:40–50
Advance Access publication 5 October 2004
doi:10.1093/rheumatology/keh414

Localization of peptidylarginine deiminase 4 (PADI4) and citrullinated protein in synovial tissue of rheumatoid arthritis

X. Chang[1], R. Yamada[1], A. Suzuki[1], T. Sawada[2], S. Yoshino[3], S. Tokuhiro[1] and K. Yamamoto[1,2]

Objectives. **Peptidylarginine deiminases (PADIs) convert peptidylarginine into citrulline via post-translational modification. Anti-citrullinated peptide antibodies are highly specific for rheumatoid arthritis (RA). Our genome-wide case–control study of single-nucleotide polymorphisms found that the PADI4 gene polymorphism is closely associated with RA. Here, we localized the expression of PADI4 and the citrullinated protein product in synovial RA tissue.**
Methods. **We used immunohistochemistry, double immunofluorescent labelling and western blotting.**
Results. **We found that PADI4 is extensively expressed in T cells, B cells, macrophages, neutrophils, fibroblast-like cells and endothelial cells in the lining and sublining areas of the RA synovium. We also found extracellular and intracellular expression of PADI4 in fibrin deposits with loose tissue structures where apoptosis was widespread. Unlike PADI4, citrullinated protein generally appeared in fibrin deposits that were abundant in the RA synovium. The citrullinated fibrin aggregate was immunoreactive against immunoglobulin (Ig) A and IgM, but not IgG and IgE. Although a little PADI4 was expressed in osteoarthritic and normal synovial tissues, significant citrullination was undetectable.**
Conclusions. **The results showed that PADI4 is mainly distributed in cells of various haematopoietic lineages and expressed at high levels in the inflamed RA synovium. The co-localization of PADI4, citrullinated protein and apoptotic cells in fibrin deposits suggests that PADI4 is responsible for fibrin citrullination and is involved in apoptosis. The immunoreactivity of citrullinated fibrin with IgA and IgM in the RA synovium supports the notion that citrullinated fibrin is a potential antigen of RA autoimmunity.**

KEY WORDS: Rheumatoid arthritis, Peptidylarginine deiminase 4 (PADI4), Citrullination, Fibrin, Synovial tissue.

Rheumatoid arthritis (RA) is a widespread autoimmune disease that is characterized by chronic joint inflammation. Serum from patients with RA contains diverse autoantibodies that constitute one primary outcome of disturbed immunoregulation [1]. In addition to rheumatoid factor (RF), anti-filaggrin autoantibody (AFA), anti-keratin antibody (AKA), anti-perinuclear factor (APF) and anti-cyclic citrullinated peptide antibody (anti-CCP) are highly specific for RA [2–6]. Recent studies indicate that the primary constituent of the B-cell epitope for AFA, AKA, APF and anti-CCP is citrulline, an amino acid metabolite of arginine [7–9]. Because of the specific anti-citrullinated protein antibodies in patients with RA, understanding protein citrullination, the enzymatic conversion of arginine to citrulline, should provide novel insights into RA pathogenesis.

Peptidylarginine deiminases (PADI) post-translationally modify peptidylarginine to citrulline in the presence of calcium ions and can change the conformation and functional properties of target proteins after citrullination [10]. To date, PADI1, PADI2, PADI3 and PADI4 have been identified in the human genome and all of them cluster on chromosome 1p36, a candidate region for RA susceptibility [11–13]. Our large-scale genome-wide case–control study using single-nucleotide polymorphisms found that a PADI4 polymorphism is distinctly associated with RA [14]. PADI4 was originally cloned from human myeloid leukaemia HL-60 cells that were exposed to the granulocyte-inducing agent retinoic acid, dimethyl sulphoxide, or the monocyte-inducing agent 1α,25-dihydroxyvitamin D3. The 2238 base pairs of PADI4 cDNA encode 663 amino acids that have 50–55% sequence identity with the other three known PADIs [15]. Immunohistochemical studies have detected PADI4 in neutrophils and eosinophils of human peripheral blood [16–18]. To understand its role in RA pathogenesis, we investigated the expression of PADI4 and the citrullinated protein in human synovial tissues and peripheral blood using immunohistochemical means. We also discuss here the possible pathway of PADI4 involvement in RA autoimmunity.

Methods and materials

Anti-PADI4 antibody preparation

We raised antisera against human PADI4 by immunizing rabbits with a synthetic oligopeptide (PAKKKSTGSSTWP, the amino acid sequence specific for the N-terminal of PADI4). The antibody was purified by affinity chromatography through a column containing histone-tagged recombinant PADI4.

[1]Laboratory for Rheumatic Diseases, SNP Research Center, Institute of Physical and Chemical Research (RIKEN), Kanagawa, [2]Department of Allergy and Rheumatology, Graduate School of Medicine, University of Tokyo and [3]Department of Joint Disease and Rheumatism, Nippon Medical School, Tokyo, Japan.

Received 19 July 2004; revised version accepted 27 August 2004.

Correspondence to: R. Yamada, Laboratory for Rheumatic Diseases, SNP Research Center, Institute of Physical and Chemical Research (RIKEN), 1-7-22 Suehiro, Tsurumi-ku, Yokohama, Kanagawa 230-0045, Japan. E-mail: ryamada@src.riken.go.jp

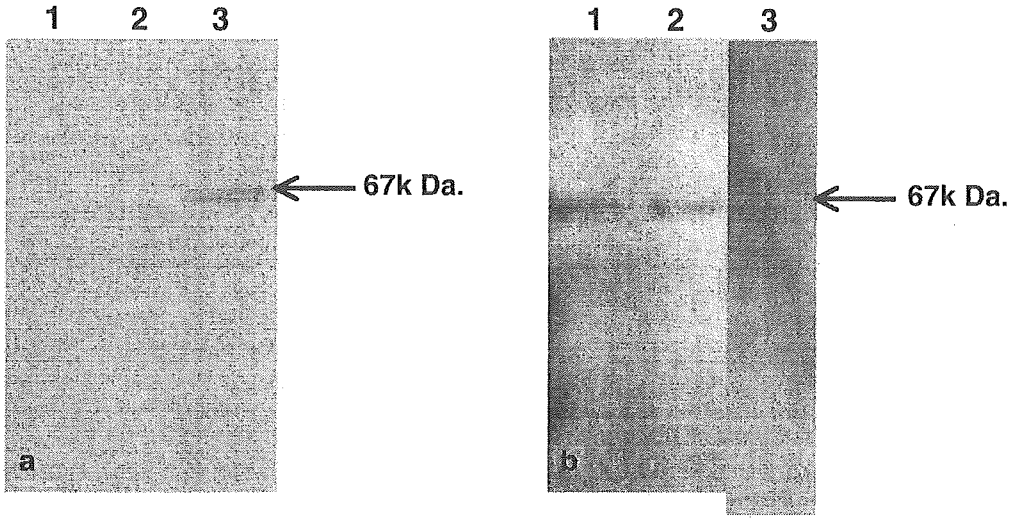

FIG. 1. PADI4 expression determined by western blotting. (a) Cultured HEK293 cells were transfected with expression vector containing coding regions of PADI4 or PADI2 or without inserts. Western blotting with anti-PADI4 antibody detected a 67-kDa band in extracts of cells expressing PADI4 (lane 3). No signals were detected in cells transfected with vector alone (lane 1) or with vector expressing PADI2 (lane 2). (b) Total proteins were extracted from RA synovial tissue (lane 1), leucocyte fraction of peripheral blood from healthy individuals (lane 2) and liver (lane 3). Western blotting shows 67-kDa PADI4 products in synovial samples but not liver samples.

Preparation of peripheral blood

Leucocytes were separated using Monopoly Resolving Medium (DaiNippon) according to the manufacturer's instructions, from samples of fresh blood obtained from 10 RA patients and nine healthy volunteers. The cells were fixed in 4% paraformaldehyde for 2 h at room temperature and then sedimented by centrifugation. Cell pellets were resuspended in phosphate-buffered saline (PBS) and spotted onto Superfrost/Plus microscope slides (Fisher).

Sample preparation of synovial and other tissues

We obtained written informed consent to collect synovial tissue samples from 12 patients with RA and five with osteoarthritis (OA) during arthroplasty. The tissues were fixed in 10% neutral buffered formalin (Sigma) for 12 h at room temperature, embedded in paraffin and sectioned by standard procedures. We also used Tissue Microarray Human Synovitis (Biocat), which includes 14 RA, 12 OA and four normal synovial tissue specimens for comparison. All RA patients met the American College of Rheumatoid Arthritis revised criteria for RA.

We determined the specificity of the PADI4 rabbit antibody and the tissue distribution of PADI4 using Vastarray (InnoGenex), a commercial tissue array slide containing normal human liver, lung, kidney, skin, muscle, brain thymus, spleen, lymph node and tonsil tissues.

Immunohistochemistry

Tissue sections were deparaffinized and rehydrated using standard procedures. Slides spotted with blood cells were processed in the same manner except for deparaffinization.

To increase immunostaining intensity, the sections were heated at 95°C for 20 min with DAKO Target Retrieval Solution (Dako). Sections were incubated with first antibody overnight at 4°C, washed three times, each for 5 min, with PBS, and then incubated with SimpleStain MAX-AP Multi (Nichirei) for 30 min at room temperature. Immunoreactive signals were visualized using the New Fuchsin Substrate kit (Nichirei) according to the manufacturer's instructions and the cell structure was defined by counterstaining with haematoxylin.

Rabbit polyclonal anti-citrulline antibody (Upstate), monoclonal anti-human fibrin (Monosan), monoclonal anti-human immunoglobulin (Ig) G Fc region, monoclonal anti-human IgM Fc region, monoclonal anti-human IgA heavy chain and monoclonal anti-human IgE Fc region (all from Zymed) were obtained commercially.

Before applying the anti-citrulline antibody, tissue sections were treated using the modification buffer supplied with the kit and then incubated with the first antibody according to the manufacturer's instructions.

Double immunofluorescent immunohistochemistry

The tissue sections were processed as described above. Monoclonal antibodies for various cell surface CD markers (CD3, CD15, CD20, CD34 or CD68) (Zymed), fibroblast-like cell marker [proxylyl 4-hydroxylase β (phβ)] (Daiichi Fine Chemicals) or Igs (IgG, IgM, IgA or IgM) (Zymed) were incubated together with rabbit antibody against PADI4 or citrulline at 4°C for 12 h. After three 5-min washes with PBS, sections were incubated with the secondary antibody for 30 min at room temperature. The monoclonal antibody and rabbit antiserum were detected using fluorescein isothiocyanate-goat anti-mouse IgG (H+L) conjugate (Zymed) and Cy™ 5-goat anti-rabbit IgG (H+L) conjugate (Zymed), respectively. Immunofluorescent signals were examined using a confocal microscope (Leica). $CD3^+$ characterized T cells, $CD20^+$ B cells, $CD15^+$ neutrophils and $CD68^+$ monocytes in peripheral blood or macrophages in tissues. $CD34^+$ identified endothelial cells or their precursors in new capillaries.

Detection of apoptosis

We detected apoptotic cells by immunohistochemistry and double immunofluorescent labelling as described above, together with use of the monoclonal antibody M30CytoDeath (Roche). This antibody can recognize a specific caspase cleavage site within

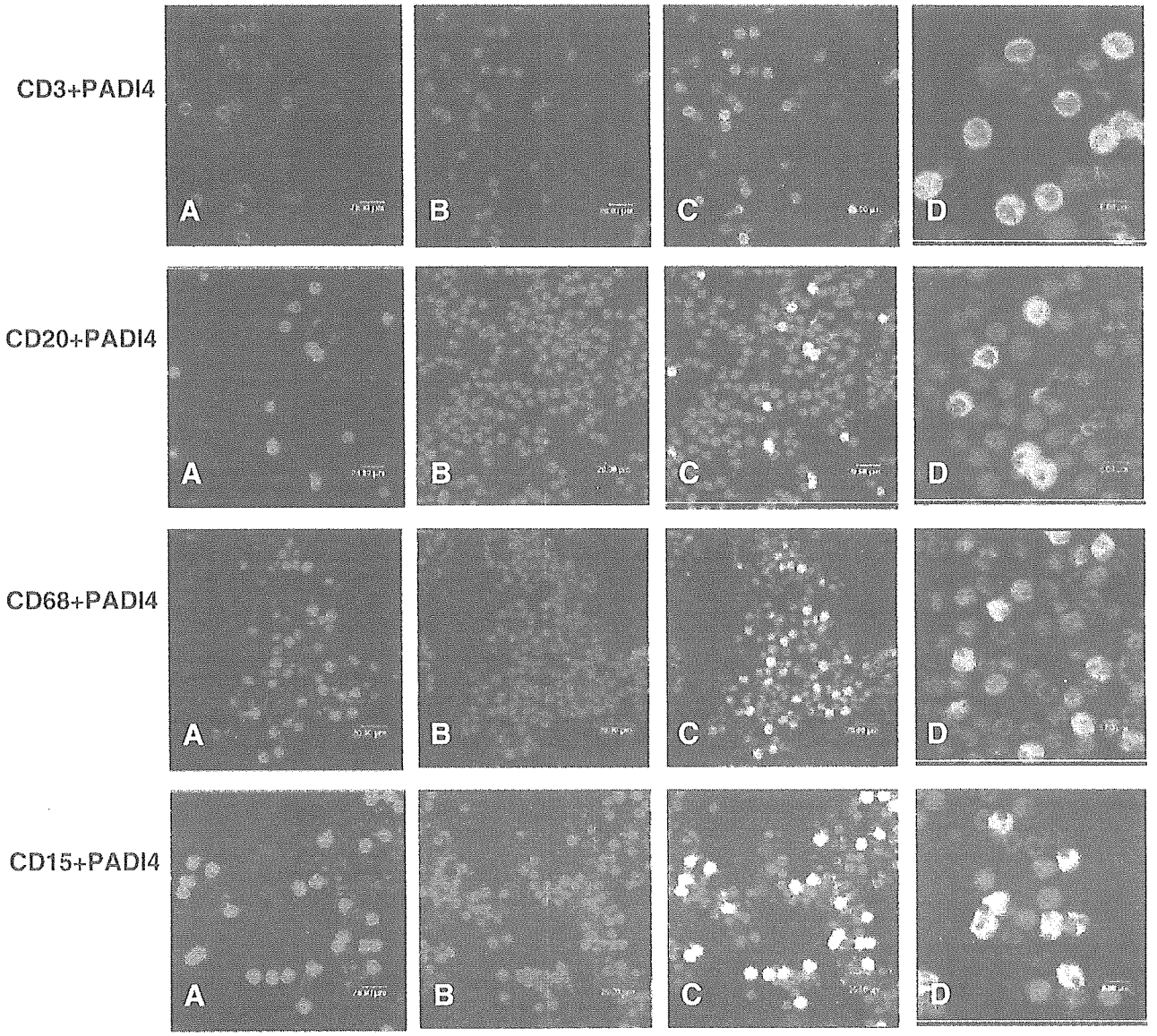

FIG. 2. Immunostaining of PADI4 in peripheral leucocytes. Peripheral leucocytes from healthy individuals were incubated with monoclonal antibodies against various cell surface CD marker and anti-PADI4 antibody. All CD-marked cells (green in A) expressed PADI4 (red in B). C, merged image of A and B; D, magnification of C. Yellow colour in merged images indicates co-localization of two protein targets. Scale bar, 20 μm in A, B and C and 8 μm in D.

cytokeratin 18 (CK18) that is not present in the native CK18 of normal cells. During the very early stage of apoptosis, caspases cleave CK18, an acidic cytokeratin intermediate filament protein of 45 kDa. The ApopDETEK Assay System (Enzo) was used to localize apoptotic cells by labelling fragmented DNA with biotinylated 16dUTP using terminal deoxynucleotide transferase. Biotinylated DNA was then visualized using the Horseradish Peroxidase-DAB *in situ* Detection System (Enzo).

Western blotting

Cultured HEK293 cells were transfected with the pTargetT™ mammalian expression vector (Promega) containing the complete PADI4 or PADI2 cDNA coding region. After a 60-h incubation, crude cellular protein was extracted by standard ultrasonic disruption. The total protein of transfected cells was separated by sodium dodecyl sulphate-polyacrylamide gel electrophoresis, transblotted onto nylon membranes and probed with anti-PADI4 antibody. A western blotting kit (KPL) was used to detect signals according to the manufacturer's instructions.

To investigate PADI4 expression in synovial tissue and peripheral leucocytes, we purified total protein of RA synovial tissues and leucocytes using total protein extraction kits (Biochain). Leucocytes were prepared using Monopoly Resolving Medium as described above. The blotted membrane was probed using our anti-PADI4 antibody and the western blot kit. The total protein in a commercial liver sample served as the control (Biochain).

Written consents was obtained from all patients and healthy volunteers according to the Declaration of Helsinki. The design of the work has been approved by the ethical committees of the

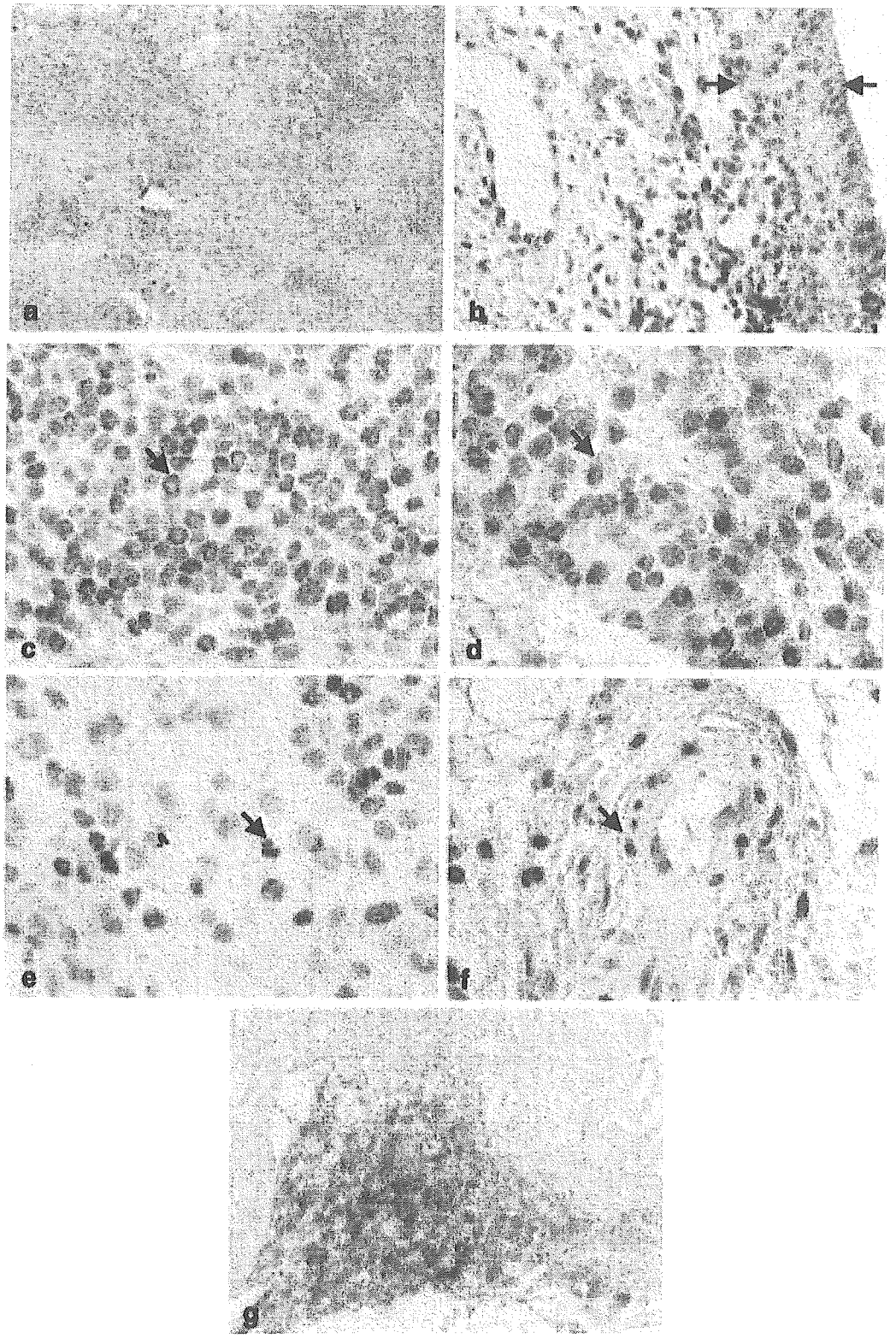

FIG. 3. Immunostaining of PADI4 in synovial RA tissue. (a) Extensive distribution of PADI4 in synovial RA tissue. (b) PADI4 is significantly expressed in the lining area marked with arrows. (c, d, e and f) Expression of PADI4 in potential lymphocytes, macrophages, polymorphic nuclear cells and capillary endothelial cells, respectively (arrows). (g) Intracellular and extracellular expression of PADI4 in loose tissue that was usually close to solid fibrin deposits and which contained cells with apoptotic morphology. Original magnification: a, 40×; b, 200×; c, d, e and f, 400×.

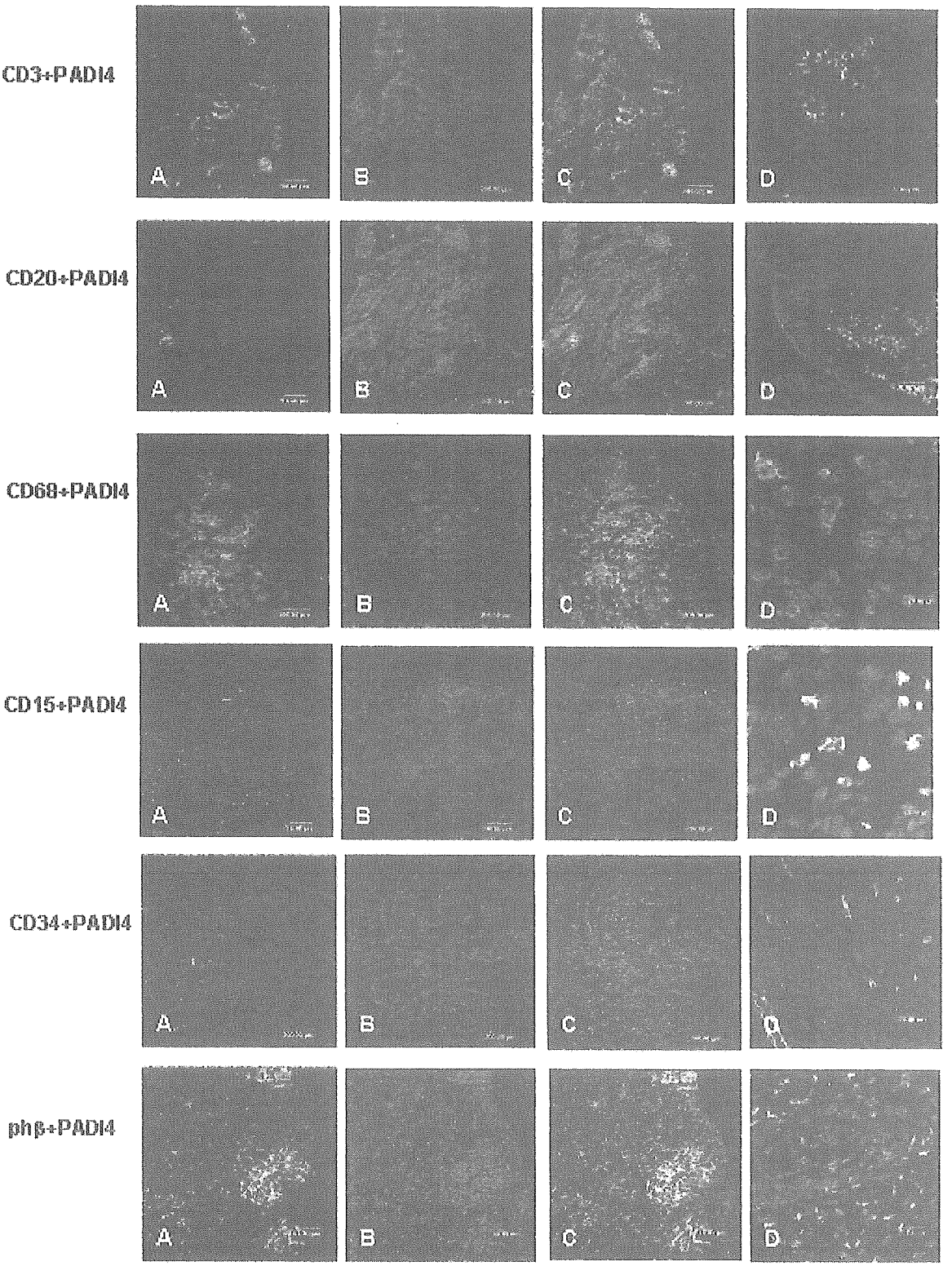

FIG. 4. Cellular distribution of PADI4 in RA synovial tissue. Synovial RA membrane was incubated with anti-PADI4 and monoclonal antibodies against leucocyte cell surface CD markers or phβ. All CD3-, CD20-, CD68-, CD15- and phβ-marked cells (green in A) expressed PADI4 (red in B). C is a merged image of A and B. D is magnification of C image. Yellow colour in merged images indicates co-localization of two protein targets. Scale bar, 200 μm in A, B and C, 20 μm in D.

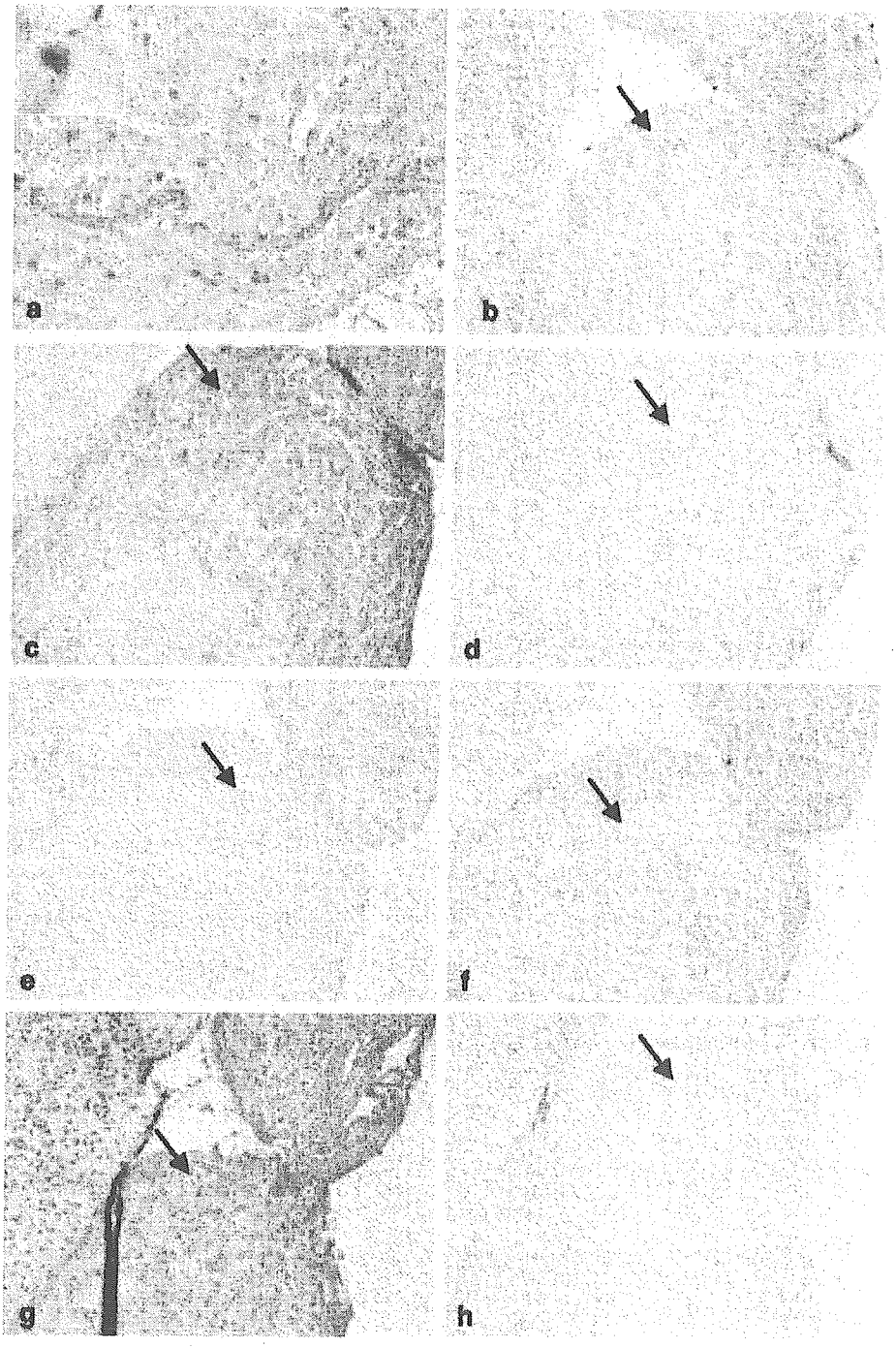

FIG. 5. Immunostaining of fibrin, citrullinated protein, PADI4, IgG, IgM, IgA and IgE in RA synovial tissue. (a) Citrullinated protein is located in some RA synovial cells in the sublining. The left upper corner is a partial magnification, indicating intracellular localization of citrullinated proteins. (b) Fibrin deposit with solid structure. (c) Citrullinated protein is located in the solid fibrin region in a continuous section. PADI4 (d) and IgG (e) were undetectable in the fibrin block. (f) Part of a solid fibrin deposit is lightly stained with anti-IgM antibody. (g) Citrullinated fibrin block was stained intensely with antibody against IgA. Capillary endothelial cells are also immunoreactive to antibody. (h) IgE was undetectable in synovial tissue. Significant IgG (i) and Ig M (j) deposits are obvious in synovial cells in the sublining of the same tissue. Arrow indicates a solid fibrin block. Original magnification: a, 400×; all other sections, 100×. (b), (c), (d), (e), (f), (g) and (h) are continuous sections. The image at the corner is shown at partial magnification.

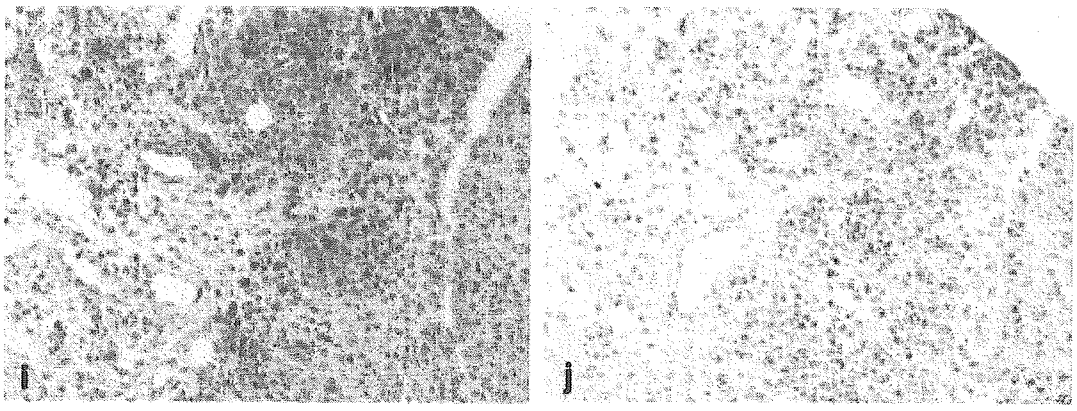

FIG. 5. Continued.

Institute of Physical and Chemical Research (RIKEN) and conforms to standards currently applied in Japan.

Results

Western blotting with PADI4 antibody

The anti-PADI4 antibody detected a band of 67 kDa in lysates of cultured HEK293 cells transfected with PADI4 expression vectors, but not in cells transfected with PADI2 or blank vector (Fig. 1a). Using the same antibody, western blotting detected a 67-kDa band in total proteins extracted from RA synovial tissue and in peripheral leucocytes of both RA patients and healthy individuals, but not in the liver of the healthy individuals (Fig. 1b). These results confirmed the specificity of our anti-PADI4 antibody. Some groups have identified a similarly sized PADI4 product in stimulated HL60 cells and in isolated synovial macrophages using an antibody against recombinant PADI4 protein [15–19].

Immunohistochemistry of PADI4 in peripheral blood cells

Double immunofluorescent labelling using anti-PADI4 antibody and antibodies against various cell surface CD markers showed that all $CD3^+$ T, $CD20^+$ B cells and $CD15^+$ granulocytes of peripheral blood expressed nuclear PADI4. $CD68^+$ monocytes also expressed nuclear and cytoplasmic PADI4 (Fig. 2). No differences were evident between samples of blood from patients with RA and healthy controls. The antibody against citrullinated protein did not detect any signals in peripheral leucocytes (data not shown).

Immunohistochemistry of PADI4 in RA synovial tissue

Immunohistochemistry with the anti-PADI4 antibody showed a broad distribution of PADI4 in many types of cells in RA synovial tissue (Fig. 3a). The lining consisted of abundant hyperplastic cells that stained intensely for PADI4 (Fig. 3b). Small mononuclear cells with little cytoplasm formed many clusters of nodular infiltrates. The nuclei of these cells were significantly stained with anti-PADI4 antibody, particularly at the nuclear edge (Fig. 3c). Large mononuclear cells with abundant cytoplasm predominated in RA synovial tissue. These macrophage-like and fibroblast-like cells were clustered in the lining and sublining of RA synovial tissue, or were dispersed in regions with a loose tissue structure. Both the cytoplasm and nuclei of these cells expressed high levels of PADI4 (Fig. 3d). In addition, polymorphonuclear cells that were evenly distributed throughout the sublining distinctly expressed nuclear PADI4 (Fig. 3e). Extensive angiogenesis is a primary feature of RA synovial tissue. The nuclei of endothelial cells surrounding small capillaries obviously expressed PADI4 peptide (Fig. 3f). PADI4 was also expressed intracellularly and extracellularly in loosely organized tissue in which the cells showed the morphology of apoptosis, having condensed chromatin, cytosol vacuolization and being separated from surrounding tissue [20] (Fig. 3g).

We investigated which type of cells contained PADI4 by double immunofluorescent labelling using an antibody for PADI4 and various CD cell markers (Fig. 4). Both $CD3^+$ T cells and $CD20^+$ B cells surrounding small capillaries expressed nuclear PADI4. The cytoplasm and nuclei of $CD68^+$ macrophages, which constitute one of the key structural components of the inflamed RA synovial membrane, expressed PADI4. $CD15^+$ cells were evenly distributed in the tissue and their polymorphic nuclei expressed PADI4. We identified angiogenic regions by detecting $CD34^+$ cells that were functional endothelial cells or the active precursors of new capillaries. The nuclei of all $CD34^+$ cells in the RA synovium were significantly immunostained with anti-PADI4 antibody. Besides, fibroblast-like cells marked with phβ antibody also expressed PADI4. The double immunofluorescent staining results were consistent with those of standard immunohistochemistry. The results were identical in all 12 of our RA samples and in 14 commercially available RA specimens.

Anti-fibrin antibody identified a significant amount of fibrin deposition in RA synovial tissues. Based on our observations, most of these fibrin deposits formed a solid block and some fibrin appeared as a mesh or spongy structure with loosely organized cells (Figs 5b and 6a). The spongiform structure, which was usually located close to the solid fibrin block, expressed large amounts of intracellular and extracellular PADI4 protein (Fig. 6c).

Immunohistochemistry of citrullinated peptides in RA synovial tissue

We immunolocalized citrullinated protein in the RA synovium using a polyclonal antibody against citrullinated peptide. Unlike the extensive distribution of PADI4, only a few synovial cells were immunostained in the sublining of the tissue (Fig. 5a). Citrullinated protein was primarily located in the solid fibrin block, which was not stained by anti-PADI4 antibody (Fig. 5b–d).

We investigated the deposition of IgG, IgM, IgA and IgE, which are central components of the autoimmune reaction, in continuous sections. Although IgG and IgM were highly immunoreactive in numerous cells at the sublining of the tissue (Fig. 5i and j), only a little fibrin deposit was mildly stained with the antibody against IgM (Fig. 5e and f). However, the citrullinated fibrin blocks in 80% of tested samples stained intensely with the antibody against IgA (Fig. 5g). IgA

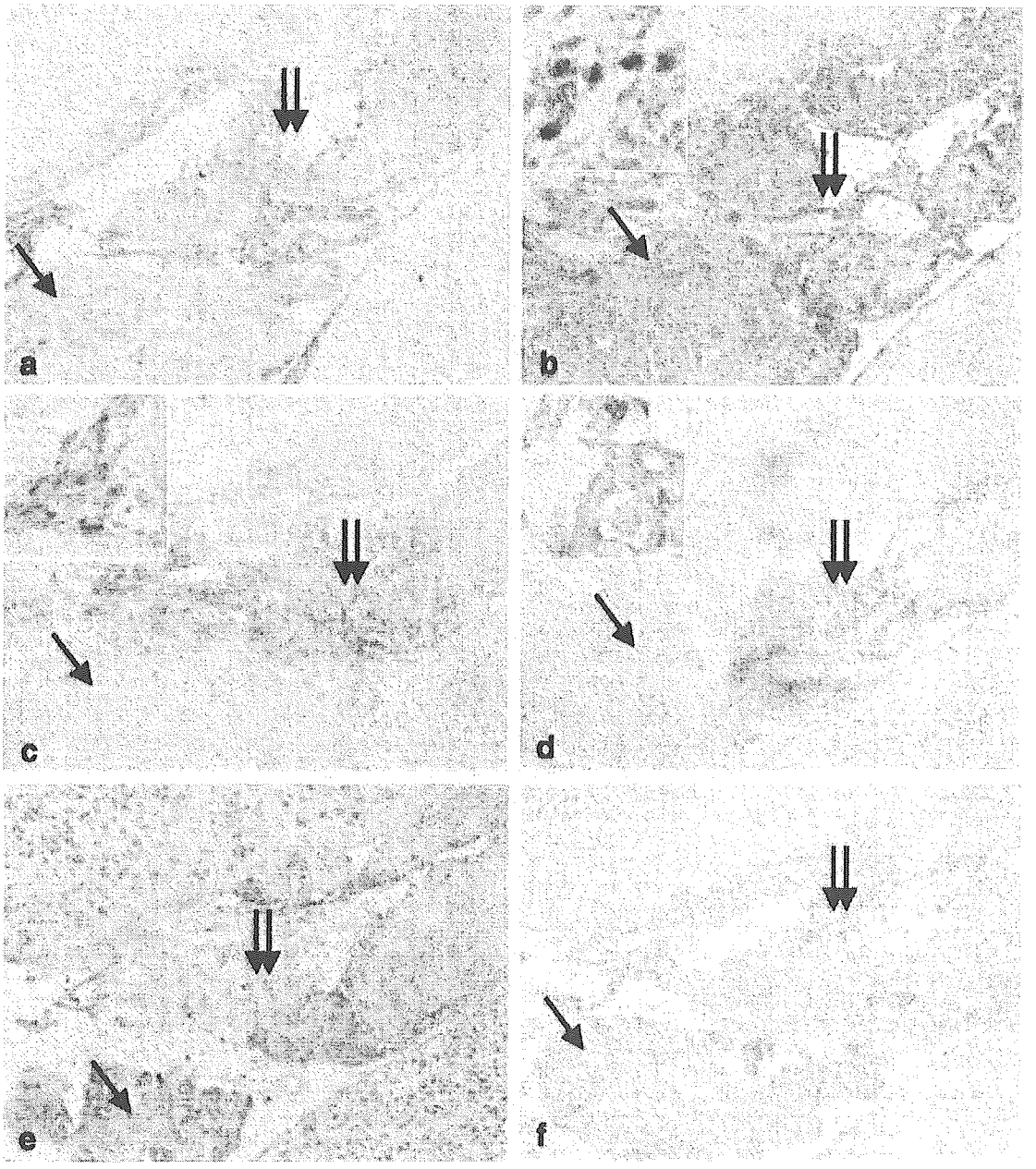

FIG. 6. Immunostaining of citrullinated protein, PADI4, apoptosis, IgG, IgM, IgA and IgE in fibrin deposits in continuous sections of RA synovial tissue. (a) A cell-loose region of RA synovial tissue was immunostained with anti-fibrin antibody. (b) Citrullinated protein is present in both solid (single arrows) and spongy (double arrows) fibrin deposits on continuous sections. (c) PADI4, (d) M30CytoDeath and fragmented DNA (e) are exclusively localized in meshed fibrin deposit. No immunosignals of IgG (f), IgM (g) and IgE (h) were evident in fibrin deposits. (i) The area of fibrin deposits is highly immunoreactive for IgA. (original magnification: (a–i), 100×). The inset images are shown at partial magnification.

immunoreaction was also detected in endothelial cells around small capillaries. The RA synovium did not express IgE immunoreactivity (Fig. 5h). These results were reproducible using anti-Ig antibodies from another manufacturer (Biomeda).

Spongiform masses that consisted of about 10% fibrin expressed intracellular citrullinated protein (Fig. 6a and b) that co-localized with PADI4 and apoptotic cells (Fig. 6c–e). Double immunofluorescent labelling also confirmed the co-localization of apoptotic cells and citrullinated protein in some fibrin deposits (results not shown). Most apoptotic cells were localized in the spongiform fibrin mass with loosely organized cells. Like the solid form, the fibrin mesh was significantly stained with antibody against IgA rather than IgG, IgM or IgE (Fig. 6f–i).

Immunohistochemistry of PADI4 in OA synovial membrane and other tissues

Immunohistochemistry using antibodies against various types of leucocytes and fibrin indicated that OA synovial tissue contains

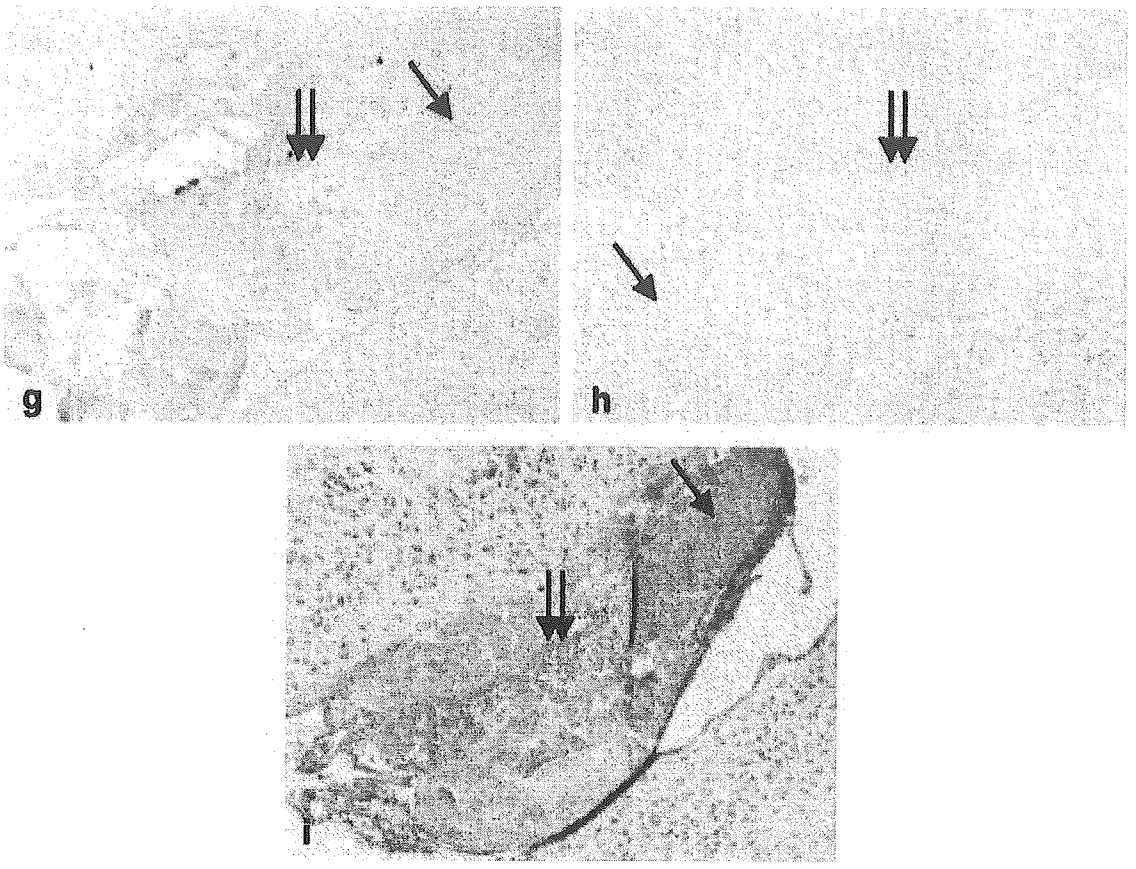

FIG. 6. Continued.

a few $CD68^+$ macrophages but lacks lymphocyte infiltrate, a hyperplastic structure and fibrin deposits. Macrophages of OA synovial tissue expressed low levels of PADI4 (Fig. 7a). Because PADI4 is mainly expressed in lymphocytes and macrophages, the loose cell structure and absence of lymphocyte infiltrate contributed to the low density of PADI4 immunostaining in OA synovial tissue. Like the findings in peripheral blood, citrullination was insignificant in OA synovial tissue (Fig. 7b). The results were similar in all 12 OA samples and in four commercially available specimens from healthy individuals.

Immunohistochemistry using the human tissue array showed distinct PADI4 expression in some regions of haematopoietic tissues, including the thymus, spleen and tonsils. The expression of PADI4 was not evident in over 30 other human tissues, including the lungs, stomach, kidneys, liver and brain (results not shown), although capillary endothelial cells and some stroma cells of these organs were stained with the anti-PADI4 antibody. Because the brain, skin and muscle express high levels of PADI1, PADI2 or PADI3 [13], the absence of immunostaining of PADI4 in these tissues further confirmed the specificity of our anti-PADI4 antibody.

In all the above experiments, no immunosignals were detected in the negative controls, which included samples with normal serum instead of the first antibody, as well as those without first or second antibodies.

Discussion

The present study provides evidence that PADI4 is expressed in peripheral blood $CD3^+$ T cells, $CD20^+$ B cells, $CD15^+$ neutrophils and $CD68^+$ monocytes. We also identified PADI4 in the same subtypes of leucocytes, fibroblast-like cells and capillary endothelial cells in RA synovial tissue. Screening over 30 normal human tissues showed selective PADI4 expression in haematopoietic tissues, including the thymus, spleen and bone marrow. Thus, we suggest that the cells expressing PADI4 in the RA synovium are mainly limited to haematopoietic cells or their derivatives. We previously detected PADI4 transcripts by northern hybridization only in haematopoietic tissues, including the spleen, thymus, peripheral blood leucocytes, fetal liver and bone marrow [14]. Mouse and rat PAD4, a homologue of human PADI4, is also expressed at high levels in granulocytes and monocytes [13, 21].

The expression of PADI4 did not differ in peripheral leucocytes from RA patients and healthy individuals. Vossenaar *et al.* also obtained similar results by reverse transcription–polymerase chain reaction and immunoblotting [19]. Moreover, we did not detect citrulline production in blood cells. These findings imply that the expression of PADI4 and its citrullination activity in the synovium both play critical roles in the pathogenesis of RA. The inflamed RA synovial membrane is formed mainly through the abnormal proliferation of macrophages and fibroblast-like cells, as well as by excessive infiltration of lymphocytes from the circulation [22]. These types of cells constitute the main source of PADI4 expression according to the present results and other studies [13, 14, 19]. Therefore, we observed extensive PADI4 expression in RA rather than OA synovial tissue or normal synovium. Vossenaar *et al.* also suggested that inflamed RA joints contain high levels of PADI peptide [19]. In addition, they localized PADI4 mRNA only in monocytes and showed that the PADI4 transcript degrades after the cells differentiate into synovial macrophages,

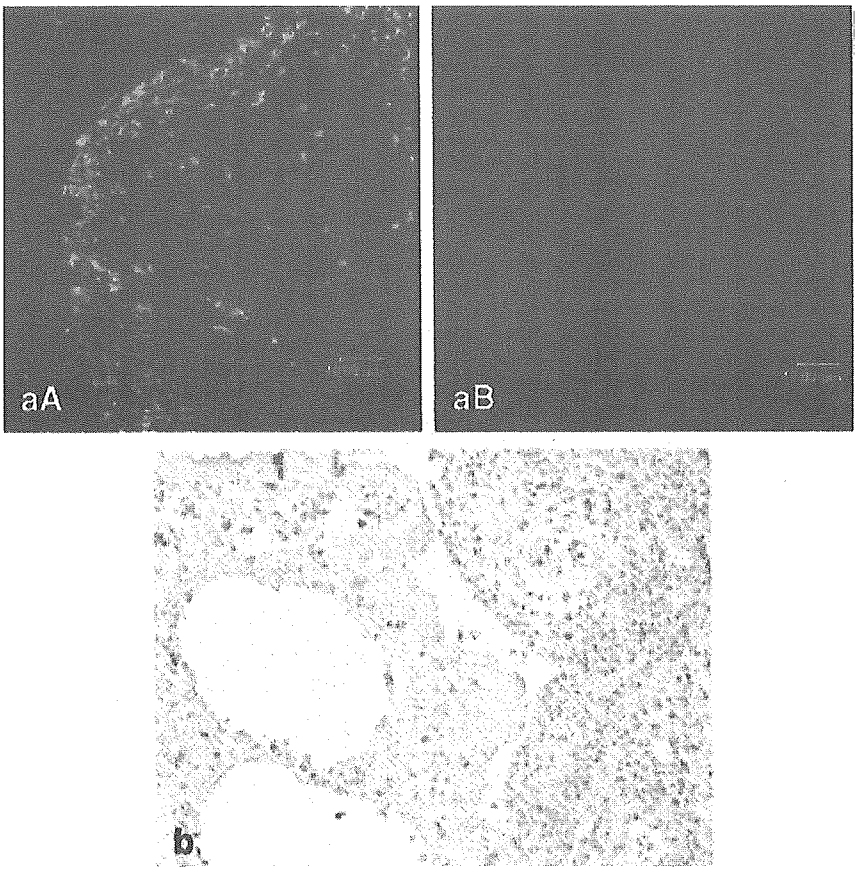

FIG. 7. Immunostaining of PADI4 and citrulline in OA synovial tissue. (a) Double immunofluorescent labelling shows CD68 macrophages (green in aA) and PADI4 signal (red in aB). Expression of PADI4 is relatively weak in macrophages of OA synovial tissue. Scale bar, 40 μm. (b) No significant immunosignals for citrullinated peptide in OA synovial tissues. Original magnification, 100×.

whereas the PADI4 protein level remains unchanged [19]. Because PADI4 transcripts with single-nucleotide polymorphisms conferring RA susceptibility have a longer half-life than non-susceptible mRNA [14], we postulate that mRNA with an RA susceptible-haplotype accumulates and becomes translated into more protein products in the RA inflamed synovium. Therefore, the high abundance of PADI4 in the synovial membrane is a prominent feature of RA pathogenesis.

Excessive fibrin formation is a prominent event of the inflamed RA joint [5, 23–25]. Amorphous fibrin deposits have been detected in the lining and deep layer of RA synovial membrane [23]. Based on our observations, fibrin aggregates appeared in the RA synovium as a solid block or as a loose tissue structure, and both forms were considerably citrullinated. However, only the loose fibrin structure expressed intracellular and extracellular PADI4. In these structures, PADI4-positive cells co-located with protein that contained citrulline, apoptotic cells that contained fragmented DNA and CK18 cleaved by caspase. Furthermore, most apoptotic cells of the RA synovium were localized in the spongiform fibrin mass. The co-localization of PADI4 and apoptotic cells in citrullinated fibrin with a loose tissue structure supports the notion that PADI4 plays a role in apoptosis and locally citrullinates fibrin, possibly by initiating apoptosis as described by Vossenaar *et al.* [19]. Then, the enzyme might leak from dead cells and continually catalyse extracellular fibrin protein. As a result, the spongy fibrin develops into a solid block after citrullination and the PADI4 enzyme is degraded extracellularly. This could explain why PADI4 expression was essentially undetectable in the solid fibrin block. In the rabbit model of antigen-induced arthritis, Sanchez-Pernaute *et al.* observed meshed fibrin at the initial stage of joint inflammation. They postulated that citrullination facilitates proteolytic fibrin cleavage and that fibrin after structural transformation activates the autoimmune reaction of RA [5, 25].

In most of the RA synovial tissue samples we tested, an antibody against IgA rather than other immunoglobulins recognized citrullinated fibrin, although some fibrin clots were also mildly immunostained with anti-IgM antibody. The IgA autoantibody has been broadly identified in rheumatoid disease. Among diverse types of RF, IgA RF is more frequently detected than IgM RF or IgG RF in the sera of individuals before a diagnosis of RA [26]. Berthelot *et al.* found the IgA class of APF in RA sera, though IgA APF was less sensitive than its classical IgG isotype [27]. Therefore, RA patients might develop an IgA class of anti-citrullinated protein antibody in response to a high concentration of citrullinated fibrin protein in the synovium. In fact, Masson-Bessiere *et al.* have reported that some fibrin in the RA synovial membrane is citrullinated and that the α and β chains of fibrin are the major targets of AFA [23]. The present study supports the notion that citrullinated fibrin triggers citrulline-specific B-cell maturation and thereby leads to RA autoimmunity [5, 23].

Although PADI4 was widely distributed in the lining and sublining of the RA synovial membrane, only a few cells of the

tissue expressed citrullinated protein. Baeten *et al.* obtained similar results using two commercially available anti-citrulline antibodies (Upstate and Biogenesis) [28]. This observation implies that the PADI4 enzyme is inactive in most RA synovial cells as well as in peripheral blood. The activation of PADI requires a high concentration of Ca^{2+} (10^{-5} mol/l) [29]. Under normal physiological conditions, the cytosolic and nucleoplasmic Ca^{2+} concentration of 10^{-7} mol/l is too low to trigger PADI enzymatic activity [19, 29]. Vossenaar *et al.* recently found that a high concentration of calcium ions induced by ionomycin could stimulate PADI and the subsequent citrullination of intracellular protein in RA synovial macrophages [19]. Ionomycin is a calcium ionophore that facilitates a sustained Ca^{2+} influx [30]. Thus, an altered level of calcium ions should explain the disparate expression of PADI4 enzyme and citrullinated peptides. However, exactly how Ca^{2+} leads to apoptosis involving PADI4 and subsequent fibrin citrullination remains unknown.

In summary, we demonstrated extensive PADI4 expression in diverse leucocyte subtypes of RA synovial tissue. We also observed significant citrullination of fibrin, as well as the co-location of PADI4, citrullinated protein and apoptosis in some fibrin deposits of the tissue. These findings might be helpful in understanding the close association of the PADI4 haplotype with RA and the important role of PADI4 in RA pathogenesis.

The authors have declared no conflicts of interest.

References

1. Corrigall VM, Panayi GS. Autoantigens and immune pathways in rheumatoid arthritis. Crit Rev Immunol 2002;22:281–93.
2. Vincent C, de Keyser F, Masson-Bessiere C, Sebbag M, Veys EM, Serre G. Anti-perinuclear factor compared with the so called antikeratin antibodies and antibodies to human epidermis filaggrin, in the diagnosis of arthritis. Ann Rheum Dis 1999;58:42–8.
3. Vencovsky J, Machacek S, Sedova L *et al.* Autoantibodies can be prognostic markers of an erosive disease in early rheumatoid arthritis. Ann Rheum Dis 2003;62:427–30.
4. Bas S, Genevay S, Meyer O, Gabay C. Anti-cyclic citrullinated peptide antibodies, IgM and IgA rheumatoid factors in the diagnosis and prognosis of rheumatoid arthritis. Rheumatology 2003;42:677–80.
5. Sanchez-Pernaute O, Largo R, Calvo E, Alvarez-Soria MA, Egido J, Herrero-Beaumont G. A fibrin based model for rheumatoid synovitis. Ann Rheum Dis 2003;62:1135–8.
6. Schellekens GA, de Jong BA, van den Hoogen FH, van de Putte LB, van Venrooij WJ. Citrulline is an essential constituent of antigenic determinants recognized by rheumatoid arthritis-specific autoantibodies. J Clin Invest 1998;101:273–81.
7. Nakamura RM. Progress in the use of biochemical and biological markers for evaluation of rheumatoid arthritis. J Clin Lab 2000;14:305–13.
8. Schellekens GA *et al.* The diagnostic properties of rheumatoid arthritis antibodies recognizing a cyclic citrullinated peptide. Arthritis Rheum 2000;43:155–63.
9. Van Venrooij WJ, Pruijn, GJ. Citrullination: a small change for a protein with great consequences for rheumatoid arthritis. Arthritis Res 2000;2:249–51.
10. Tarcsa E *et al.* Protein unfolding by peptidylarginine deiminase. Substrate specificity and structural relationships of the natural substrates. J Biol Chem 1996;271:30709–16.
11. Cornelis F *et al.* New susceptibility locus for rheumatoid arthritis suggested by a genome-wide linkage study. Proc Natl Acad Sci USA 1998;95:10746–50.
12. Shiozawa S *et al.* Identification of the gene loci that predispose to rheumatoid arthritis. Int Immunol 1998;10:1891–95.
13. Vossenaar ER, Zendman AJW, van Venrooij WJ, Pruijn GZM. PAD, a growing family of citrullinating enzymes: genes, features and involvement in disease. Bioassay 2003;25:1106–18.
14. Suzuki A *et al.* Functional haplotypes of PADI4, encoding citrullinating enzyme peptidylarginine deiminase 4, are associated with rheumatoid arthritis. Nat Genet 2003;34:395–402.
15. Nakashima K, Hagiwara T, Ishigami A *et al.* Molecular characterization of peptidylarginine deiminase in HL-60 cells induced by retinoic acid and 1alpha, 25-dihydroxyvitamin D(3). J Biol Chem 1999;274: 27786–92.
16. Asaga H, Nakashima K, Senshu T, Ishigami A, Yamada M. Immunocytochemical localization of peptidylarginine deiminase in human eosinophils and neutrophils. J Leukoc Biol 2001;70:46–51.
17. Hagiwara T, Nakashima K, Hirano H, Senshu T, Yamada M. Deimination of arginine residues in nucleophosmin/B23 and histones in HL-60 granulocytes. Biochem Biophys Res Commun 2002;290:979–86.
18. Nakashima K, Hagiwara T, Yamada M. Nuclear localization of peptidylarginine deiminase V and histone deimination in granulocytes. J Biol Chem 2002;277:49562–8.
19. Vossenaar ER, Radstake TR, Van Der Heijden A *et al.* Expression and activity of citrullinating peptidylarginine deiminase enzymes in monocytes and macrophages. Ann Rheum Dis 2004;63:373–81.
20. Hacker G. The morphology of apoptosis. Cell Tissue Res. 2000; 301:5–17.
21. Vossenaar ER, Nijenhuis S, Helsen MM *et al.* Citrullination of synovial proteins in murine models of rheumatoid arthritis. Arthritis Rheum 2003;48:2489–500.
22. Cutolo M, Sulli A, Barone A, Seriolo B, Accardo S. Macrophages, synovial tissue and rheumatoid arthritis. Clin Exp Rheumatol 1993;11:331–9.
23. Masson-Bessiere C, Sebbag M, Girbal-Neuhauser E *et al.* The major synovial targets of the rheumatoid arthritis-specific antifilaggrin autoantibodies are deiminated forms of the alpha- and beta-chains of fibrin. J Immunol 2001;166:4177–84.
24. Weinberg JB, Pippen AM, Greenberg CS. Extravascular fibrin formation and dissolution in synovial tissue of patients with osteoarthritis and rheumatoid arthritis. Arthritis Rheum 1991;34:996–1005.
25. Sanchez-Pernaute O, Lopez-Armada MJ, Calvo E *et al.* Fibrin generated in the synovial fluid activates intimal cells from their apical surface: a sequential morphological study in antigen-induced arthritis. Rheumatology 2003;42:19–25.
26. Rantapaa-Dahlqvist S, de Jong BA, Berglin E *et al.* Antibodies against cyclic citrullinated peptide and IgA rheumatoid factor predict the development of rheumatoid arthritis. Arthritis Rheum 2003;48: 2741–9.
27. Berthelot JM, Bendaoud B, Maugars Y, Audrain M, Prost A, Youinou P. Antiperinuclear factor of the IgA isotype in active rheumatoid arthritis. Clin Exp Rheumatol 1994;12:615–9.
28. Baeten D, Peene I, Union A *et al.* Specific presence of intracellular citrullinated proteins in rheumatoid arthritis synovium: relevance to antifilaggrin autoantibodies. Arthritis Rheum 2001;44:2255–62.
29. Inagaki M, Takahara H, Nishi Y, Sugawara K, Sato C. $Ca2^{+}$-dependent deimination-induced disassembly of intermediate filaments involves specific modification of the amino-terminal head domain. J Biol Chem 1989 25;264:18119–27.
30. Schwab BL, Guerini D, Didszun C *et al.* Cleavage of plasma membrane calcium pumps by caspases: a link between apoptosis and necrosis. Cell Death Differ 2002;9:818–31.

Genes and Immunity (2005) 6, 194–202

www.nature.com/gene

FULL PAPER

CUL1, a component of E3 ubiquitin ligase, alters lymphocyte signal transduction with possible effect on rheumatoid arthritis

R Kawaida[1,3], R Yamada[1], K Kobayashi[1], S Tokuhiro[1,3], A Suzuki[1], Y Kochi[1,2], X Chang[1], A Sekine[1], T Tsunoda[1], T Sawada[2], H Furukawa[3], Y Nakamura[1] and K Yamamoto[1,2]

[1]*SNP Research Center, RIKEN, Yokohama, Kanagawa, Japan;* [2]*Graduate School of Medicine, University of Tokyo, Tokyo, Japan;* [3]*Biomedical Research Laboratories, Sankyo Co., Ltd, Tokyo, Japan*

Ubiquitination affects various immune processes and E3 ubiquitin ligases (E3) play an important role in determining substrate specificity. We identified 11 human E3 ligase genes of potential importance in pathogenesis of autoimmune diseases by search of public databases and screened them for candidacy of biological investigation with case–control linkage disequilibrium tests on multiple SNPs in the genes using rheumatoid arthritis (RA) as a model of autoimmune diseases. Significant association with RA was observed in an SNP in intron 3 of Cullin 1 (CUL1) that affected transcriptional efficiency of the promoter activity in lymphocytic cell lines. Quantitative expression analysis revealed that CUL1 mRNA was highly detected in lymphoid tissues including spleen and tonsil, and was specifically expressed in T and B lymphocytes in fractionated peripheral leukocytes. Histological evaluation of tonsils indicated that CUL1 protein expression was relatively specific for maturing germinal centers. Suppression of CUL1 expression had influence on the phenotype of T-cell line, that is, it inhibited IL-8 induction, which is known to play an important role in the migration of inflammatory cells into the affected area seen in RA. Our data suggest that the regulation of CUL1 expression in immunological tissues may affect the susceptibility of RA via altering lymphocyte signal transduction.

Genes and Immunity (2005) **6**, 194–202. doi:10.1038/sj.gene.6364177
Published online 10 March 2005

Keywords: *rheumatoid arthritis; SNP; Cullin1; E3 ubiquitin ligase*

Introduction

The ubiquitin system contributes to many aspects of cellular activities. The length of the ubiquitin chain is generally related to different processes. Whereas at least four units of the ubiquitin chain seem necessary for proteasomal degradation,[1] mono-ubiquitination is involved in endocytosis.[2] The ubiquitin–proteasome system degrades polyubiquitinated proteins via the 26S protein complex, the proteasome. The machinery contributes to a variety of cellular processes, including cell-cycle control, signal transduction, transcriptional regulation, DNA repair, antigen presentation and apoptosis.[3] In addition to physiologically normal proteins, misfolded proteins could be substrates in the cellular stress response, through which E3s constitute a protein quality control system.[4] However, other regulatory roles such as internalization of the receptor protein,[5–7] transcription stimulation[8,9] and protein processing[10,11] via ubiquitination have recently been suggested.

Ubiquitin is a small peptide of 76 amino acids that is highly conserved in all eukaryotes. The ubiquitin pathway proceeds through a three-step enzymatic cascade involving ubiquitin-activating enzyme (E1), ubiquitin-conjugating enzyme (E2) and ubiquitin ligase (E3). While there are only dozens of E2s, E3s are highly heterogeneous. This feature allows these enzymes to determine specific ubiquitin interactions with its target proteins[12] that control cell processes such as activation, proliferation and differentiation.

The ubiquitination system is also involved in many aspects of the immune system. For example, antigens processed by polyubiquitination are presented on the surfaces of antigen-presenting cells (APCs) that are recognized by MHC class I molecules of cytotoxic T cells. Proteasome and tripeptidyl aminopeptidase II (TPPII) might cooperate to produce peptides bound by MHC class I proteins.[13,14]

E3 ubiquitin ligases are also involved in the NF-κB signaling pathway that regulates the expression of various genes during inflammation, immunity, differentiation and apoptosis. The activation cascade is also modulated by the multiple ubiquitination system

Correspondence: Dr R Yamada, Laboratory for Rheumatic Diseases, SNP Research Center, Institute of Physical and Chemical Research, 1-7-22 Suehiro-cho, Tsurumi-ku, Yokohama, Kanagawa 230-0045, Japan.
E-mail: ryamada@src.riken.go.jp
Received 15 November 2004; revised 3 January 2005; accepted 4 January 2005; published online 10 March 2005

executed by E3s. In response to proinflammatory cytokines, TRAF6 modified by polyubiquitin chains is essential for TAK1 kinase activation, which leads to IκB kinase (IKK) phosphorylation.[15,16] The activation of IKK causes the phosphorylation and degradation of IκBα, followed by NF-κB activation. The SCF (Skp1–Cullin1–Fbox)$^{\beta\text{-TrCP}}$ E3 complex participates in IκBα degradation.[17,18] Furthermore, another ubiquitin ligase might execute the proteolysis of NF-κB p105 into active subunits to translocate into the nucleus and regulate target gene transcription.[19] Recently it has been found that adaptor protein Bcl10, which is essential for NF-κB activation by T- and B-cell receptors, promotes NF-κB activation through the paracaspase- and UBC13-dependent ubiquitination of NEMO (IKK-γ).[20]

Some E3s play regulatory roles in T-cell anergy. For example, GRAIL suppresses and limits activation-induced IL-2 and IL-4 production in T-cell hybridomas.[21] The constitutive expression of GRAIL renders naive CD4T cells anergic.[22] T cells derived from E3 Itch$^{-/-}$ mice are activated and their proliferation is enhanced, which results in severe immune and inflammatory disorders and constant itching of the skin.[23] Furthermore, c-Cbl and Cbl-b negatively regulate T-cell activation by promoting the clearance of engaged TCR from the cell surface by ubiquitination,[24] and Cbl-b negatively regulates BCR signaling by targeting Syk for ubiquitination.[25]

As shown above, E3s are involved in immune processes. We identified CUL1 among E3s as a candidate of autoimmunity-related gene by screening association between SNPs and rheumatoid arthritis (RA). RA is a widespread autoimmune disease that affects 0.5–1.0% of the worldwide population. It is characterized by chronic inflammation of the synovial joints due to the infiltration of lymphocytes, macrophages and plasma cells, accompanied by hyperplasia of the synovial fibroblasts. The pathology of RA is generally defined by the activities of many inflammatory cytokines. The ubiquitin system might be involved in RA because the overexpression of the E3 ubiquitin ligase, Synoviolin/Hrd1, causes the excessive growth of synoviocytes in mice, which leads to spontaneous arthropathy.[26] One risk factor for RA is genetic contribution. The susceptibility of siblings of affected individuals and of monozygotic twins is higher than that of the general population. Genetic studies of RA using SNPs have revealed RA-susceptible SNPs such as PADI4,[27] RUNX1 and SLC22A4,[28] and PTPN22.[29] Therefore, to identify the E3s involved in autoimmune diseases, we performed a case–control linkage disequilibrium study of the Japanese RA population. We discovered an SNP associated with RA in *CUL1*, a component of the SCF E3 complex.

CUL1 is highly conserved from nematodes to humans,[30] and it is indispensable for mouse embryogenesis.[31] CUL1 binds to the Skp1–F-box protein complex and to ROC1 through its N- and C-terminal region, respectively. F-box is a member of a large family of substrate-targeting proteins that determine the specificity of E3 activity. ROC1, on the other hand, recruits an E2 enzyme and functions as a ubiquitin ligase on its substrate.[32] A structural characteristic of the E3 ligase is the RING finger motif in ROC1.[33] Besides IκBα,[17,18] SCF complex has several targets, including β-catenin,[16] p27, CyclinE1[34] and IFNα receptor 1.[6] Thus, SCF has been studied as an inflammation or/and cell cycle modulator. Here, we analyze the expression and function of CUL1 in the context of the immune system in autoimmunity.

Results

Analysis of RA-related SNPs in E3 ubiquitin ligase

Screening of E3 ubiquitin ligase genes for association with RA with SNPs. A total of 11 E3 ubiquitin ligase genes were selected as described in Materials and methods. Table 1 lists the SNPs and the genotyping results. All the SNPs were polymorphic in Japanese population, with a minor allele frequency more than 0.08% except for #31 in GRAIL. Among 33 SNPs in the 11 selected genes, only one SNP (#8) in intron 3 of the *CUL1* gene was significantly associated with RA, with $P<0.0005$ (corrected $P<0.05$ by Bonfferoni correction). Based on these results, we selected CUL1 for further analysis for function and mechanism in immune system.

SNP mapping in CUL1 locus. To investigate the region around *CUL1*, we analyzed the LD and haplotype structure with the genotype data of 40 SNPs for 94 case samples (Figure 1). SNPs with a moderately strong LD ($\Delta>0.5$) to #8 were distributed in both *CUL1* and its neighboring gene *EZH2*. We then searched for SNPs in this region using the JSNP database, which mainly focuses on SNPs in the 5′UTR, 3′UTR and the coding region.[35] We also directly sequenced 2 kb of the 5′-flanking region and exon 1, in 48 genomic samples from RA patients to find functional SNPs in the promoter region. Thus, among 40 genotyped SNPs, only intron 3 of *CUL1* contained SNPs with a *P*-value of <0.001. Furthermore, no SNPs were associated with RA in the *CUL1* coding, or 5′ and 3′ flanking regions (Figure 1). Therefore, SNP #8 in intron 3 of *CUL1* could affect susceptibility to RA. We therefore examined the functional differences of associated SNP #8.

Reporter assay of RA-associated SNP in CUL1. Reporter constructs containing one, five or nine concatenated copies of the 24 nucleotides around the associated SNP #8 were connected to the SV40 promoter (Figure 2a). The constructs were transiently transfected into both the Jurkat T-cell (Figure 2b) and Raji B-cell (Figure 2c) lines. The susceptible C allele had more enhancer activity than the nonsusceptible A allele in both cell lines, with statistical significance $P<0.005$ for five and nine concatenated constructs.

Expression of CUL1

Quantitative RT-PCR. To elucidate the role of CUL1 in inflammatory disease, we analyzed the mRNA expression level using quantitative real-time PCR. The expression levels of *CUL1* mRNA in a human tissue panel were high in the spleen, tonsils and in whole blood, and moderate in the brain, thymus, bone marrow and liver. The kidneys and heart expressed low levels of *CUL1* mRNA (Figure 3a). Synovial fibroblast cells from RA patients also expressed moderate levels of *CUL1*. Mononuclear cells in the peripheral blood expressed more *CUL1* mRNA than polynuclear cells and lymphocyte-dominant expression of CUL1 was further ascertained with expression evaluation of fractionated cells stratified with cell surface markers CD4, 8, 14 and 19 (Figure 3b).

Table 1 Summary of association of selected SNPs in E3 ubiquitin ligase between cases and controls

JSNP ID[a]	*dbSNP ID*[b]	*Chromosome*	*Public location*[c]	*SNP_ID*	*Gene_name*	*Refseq*	*Structure*	*Case*				*Control*				*Allele 1 vs allele 2 P*	*Genotype 11 vs 12+22 P*	*Genotype 22 vs 11+12 P*
								11	*12*	*22*	*Sum*	*11*	*12*	*22*	*Sum*			
IMS-JST084689	rs3738885	2		#1	BARD1	NM_000465.1	exon	0	57	746	803	2	39	616	657	0.6825	0.1177	0.5146
IMS-JST123390	rs3768710	2		#2	BARD1	NM_000465.1	intron	311	355	140	806	225	325	108	658	0.3457	0.0828	0.6275
IMS-JST123387	rs3768707	2		#3	BARD1	NM_000465.1	intron	56	274	471	801	41	237	367	645	0.6931	0.6315	0.4664
IMS-JST129605	rs3774206	3		#4	VHL	NM_000551.2	3′UTR	524	269	32	825	411	209	29	649	0.7949	0.9410	0.5726
—	rs1678607	3		#5	VHL	NM_000551.2	intron	522	271	32	825	408	213	28	649	0.7785	0.8724	0.6744
—	—	3	10172799	#6	IRAK2|VHL	NM_000551.2	intergene	0	3	822	825	0	3	645	648	0.7666	1.0000	0.7664
IMS-JST166832	rs243505	7		#7	CUL1	NM_003592.2	intron	401	354	69	824	299	267	84	650	0.0362	0.3090	0.0045
IMS-JST159456	rs243480	7		#8	CUL1	NM_003592.2	intron	89	378	355	822	109	298	237	644	0.0005	0.0007	0.0134
IMS-JST166838	rs3807447	7		#9	CUL1	NM_003592.2	intron	9	127	684	820	6	96	536	638	0.7194	0.7680	0.7593
IMS-JST008077	rs2072173	7		#10	SMURF1	NM_020429.1	intron	375	331	82	788	309	239	69	617	0.6258	0.3536	0.6407
IMS-JST008078	rs219797	7		#11	SMURF1	NM_020429.1	exon	350	323	108	781	249	259	89	597	0.2550	0.2491	0.5705
IMS-JST159788	rs3801241	7		#12	SMURF1	NM_020429.1	intron	63	314	430	807	47	251	358	656	0.5576	0.6432	0.6227
		8	87325448	#13	WWP1	NM_007013.3	intron	3	100	720	823	2	72	573	647	0.5268	0.8563	0.5285
—	—	8	87319229	#14	WWP1	NM_007013.3	intron	380	359	86	825	270	289	90	649	0.0245	0.0870	0.0430
—	—	8	87331177	#15	WWP1	NM_007013.3	intron	285	397	143	825	194	311	144	649	0.0097	0.0583	0.0195
IMS-JST027139	rs2279434	10		#16	c-MIR	NM_145021.2	intron	15	161	633	809	19	142	493	654	0.1137	0.1846	0.1961
IMS-JST064533	rs2306814	10		#17	c-MIR	NM_145021.2	intron	0	47	760	807	0	49	605	654	0.2085	1.0000	0.2006
IMS-JST118972	rs3764990	10		#18	c-MIR	NM_145021.2	exon	12	162	623	797	12	145	491	648	0.2640	0.6086	0.2810
IMS-JST032946	rs2283428	15		#19	UBE3A	NM_000462.2	intron	0	6	778	784	0	2	530	532	0.3732	1.0000	0.3725
—	—	15	23147683	#20	UBE3A	NM_000462.2	intron	333	373	119	825	261	300	87	648	0.7989	0.9734	0.5834
—	—	15	23218664	#21	UBE3A	NM_000462.2	intron	120	374	330	824	88	300	261	649	0.7438	0.5829	0.9482
IMS-JST100147	rs3748401	16		#22	AMFR	NM_001144.3	exon	6	105	682	793	4	85	568	657	0.7568	0.7350	0.8042
IMS-JST100149	rs2617846	16		#23	AMFR	NM_001144.3	intron	221	383	202	806	181	330	146	657	0.4239	0.9558	0.2045
IMS-JST100150	rs2617847	16		#24	AMFR	NM_001144.3	intron	108	348	254	710	56	188	132	376	0.9367	0.8894	0.8267
IMS-JST039538	rs2288339	17		#25	SMURF2	NM_022739.2	intron	23	220	545	788	19	129	348	496	0.9771	0.3711	0.7049
IMS-JST060286	rs2303572	17		#26	SMURF2	NM_022739.2	intron	712	40	0	752	476	28	1	505	0.6425	0.7466	0.2222
IMS-JST060287	rs2303573	17		#27	SMURF2	NM_022739.2	intron	692	43	0	735	463	29	0	492	0.9748	0.9744	1.0000
IMS-JST114708	rs3761147	20		#28	ITCH	NM_031483.3	intron	367	342	97	806	284	306	60	650	0.7837	0.4824	0.0864
—	rs2424992	20		#29	ITCH	NM_031483.3	intron	373	352	99	824	290	283	75	648	0.9833	0.8440	0.7950
—	rs3746455	20		#30	ITCH	NM_031483.3	UTR 5	373	351	99	823	292	281	75	648	0.9556	0.9207	0.7885
—	rs5962358	X		#31	GRAIL	NM_194463.1	intron	823	0	0	823	645	0	0	645	N. D.	1.0000	1.0000
—	rs6523888	X		#32	GRAIL	NM_194463.1	intron	0	3	821	824	0	1	646	647	0.4440	1.0000	0.4437
—	rs2880013	X		#33	GRAIL	NM_194463.1	intron	456	266	103	825	410	134	105	649	0.2050	0.0022	0.0432

[a]JSNP database.
[b]National Center for Biotechnology Information (NCBI) dbSNP database.
[c]Location of SNP based on chromosomal data in Build34.